

*I would like to dedicate my thesis to  
my beloved parents.*

# Acknowledgement

First of all, praise be to ALLAH the Great and Omnipotent surrounded me under his guidance during MS study, in the School of Chemical and Material Engineering (SCME), National University of Science and Technology (NUST).

I would like to express my utmost gratefulness to my supervisor Dr. Nasir Mehmood Ahmad for his valuable supervision, guidance and commitments in experimental work and thesis writing. He has been a consistent source of motivation and support. I am thankful to Dr. Zakir Hussain for his never-ending support in different situations. I thank him for his concern in my research project. I am grateful to Dr. Nabeel Anwar for his suggestion during my experimental and thesis work.

I would like to express my gratitude to Dr. Zakir Hussain (SCME) and Dr. Nosheen Fatima (SMME) for helping in project and all the supporting and cooperative staff members of research laboratories visited during the project including SCME, SMME and SNS. In particular, I would like to be thankful to Zafar Iqbal and Shamas Uddin in helping me in dealing with the situation and guiding me during the experimental work.

I would like to thank my lab mates and my friends Muhammad Zakir Hussain, Zarrar Khan, Abrar Khattak and Sheraaz tariq for never ending support. I am grateful to Asra Tariq for guiding in writing in my thesis.

Above all, I want to express my love to my family. I must thank to my mother Naseem Zahra and father Zamir ul Hassan for never ending support and guidance. They encouraged me not to leave a job in hard situation. They always motivated me to see the brighter side of situation. They are always a source of inspiration for me. A special thanks to my siblings for always helping me and being my best friend.

*Muhammad Asad Abbas*

# Abstract

Current study is about the grafting of PtBA polymer brushes on the Surface of TFC PA membrane via ATRP which took place through four phases namely functionalization of TFC PA by APTMS, bromination of APTMS functionalized membrane, growth of PtBA polymer brushes on TFC PA membrane and then the hydrolysis of polymer brushes grown membrane. Contact angle analysis, optical profilometry and FTIR analysis has been done at each step of grafting. Morphology, permeation flux, salt rejection and pore size was investigated. The contact angle for water has been reduced from  $51^\circ$  to  $34^\circ$  due to conversion of PtBA to PAA which results in increase in hydrophilicity. The flux rate has also been increased from  $75 \text{ L/m}^2\cdot\text{hr}$  to  $80 \text{ L/m}^2\cdot\text{hr}$  at pH 3. Salt rejection is lowered from 98.8 to 95% but it remains in the acceptable range. The result membrane has better hydrophilicity and permeation flux. The tensile testing of membrane has shown that due to the grafting of PAA on the membrane surface, the mechanical strength of the membrane has been increased appreciable.

# Table of Contents

TH 1 form.....	ii
TH 4 form.....	iii
Thesis acceptance certificate.....	iv
Dedication.....	v
Acknowledgement.....	vi
Abstract.....	vii
Table of Contents .....	viii
List of figures .....	xii
List of tables .....	xiv
List of Abbreviations .....	xv
Chapter 1: Introduction.....	1
1.1 Background:.....	1
1.2 Water pollution in Pakistan: .....	1
1.3 Emergence of Polymeric membrane:.....	2
1.4 Membrane fouling: .....	2
1.5 Research framework: .....	4
1.6 Aims and objectives:.....	4
Chapter 2: Literature Review .....	6
2.1 Membrane technology: .....	6
2.1.1 What is membrane technology:.....	6
2.2 Types of membrane separation processes:.....	6
2.2.1 Pressure driven membrane processes:.....	6
2.2.2 Electrically driven membrane processes:.....	7
2.2.3 Novel membrane processes:.....	8

2.3 Membrane technology for water treatment:.....	8
2.3.1 Microfiltration: .....	9
2.3.2 Ultrafiltration: .....	9
2.3.3 Nanofiltration: .....	9
2.3.4 Reverse Osmosis membrane: .....	9
2.4 Thin film composite polyamide membrane: .....	12
2.5 Methods for the modification of PA membrane: .....	13
2.5.1 Bulk modification: .....	14
2.5.2 Blending methods: .....	14
2.5.3 Surface-coating TFC-PA membrane:.....	15
2.5.4 Surface coating via interfacial polymerization: .....	15
2.5.5 Photo-induced grafting PA membrane:.....	15
2.5.6 Gamma ray and electron/ion beam-induced grafting TFC-PA membranes:..	16
2.5.7 Plasma treatment and plasma-induced grafting polymerization: .....	16
2.5.8 Thermal induced grafting and immobilization:.....	17
2.5.9 Initiated chemical vapour deposition method: .....	17
2.5.9 Surface Initiated ATRP:.....	17
2.6 Atomic transfer radical polymerization ATRP:.....	17
2.6.1 General mechanism of ATRP: .....	18
2.6.2 Components of normal ATRP:.....	19
2.7 Polymer brushes:.....	21
2.7.1 Why to choose ATRP for polymer brushes: .....	22
2.7.2 Controlled synthesis of polymer brushes by ATRP (SI-ATRP):.....	22
2.7.3 Applications of polymer brushes: .....	23
Chapter 3: Materials and Experimental Work.....	24

3.1 Materials: .....	24
3.2 Experimental work:.....	24
3.2.1: Functionalization of TFC RO membrane with APTMS: .....	25
3.2.2 Initiator attachment on APTMS functionalized TFC RO membranes:.....	26
3.2.3 Polymer brushes grafting (preparation of TFC PA-tBA membranes): .....	26
3.2.4 Hydrolysis of polymer brush grafted membrane: .....	28
Chapter 4: Characterization techniques.....	29
4.1 FTIR-ATR: .....	29
4.1.1 Introduction:.....	29
4.1.2 Working of FTIR-ATR: .....	29
4.1.3 FTIR-ATR of membrane samples:.....	30
4.2 Scanning electron microscopy: SEM.....	30
4.2.1 Introduction: .....	30
4.2.2 Construction: .....	31
4.2.3 Interaction of electrons with matter: .....	32
4.2.4 SEM of membrane samples .....	34
4.3 Contact Angle Analysis: .....	34
4.3.1 Introduction:.....	34
4.3.2 Measurement of contact angle: .....	34
4.4 Optical profilometry: .....	35
4.4.1 Introduction .....	35
4.4.2 Working of optical profilometry: .....	35
4.4.3 Optical profilometry of membrane samples:.....	36
4.5 Optical microscopy:.....	37
4.5.1 Introduction:.....	37

4.5.2 Working: .....	37
4.5.3 Optical microscopy of membrane sample:.....	37
4.6 Permeation flux:.....	38
CHAPTER 5: Results and discussions .....	39
5.1: Reaction scheme for the synthesis of polymer brushes: .....	39
5.1.1 Reaction of TFC PA membrane with APTMS: .....	39
5.1.2 Reaction of $\alpha$ -bromo isobutyl with APTMS functionalized TFC PA membrane:.....	40
5.1.3 PtBA brushes growth on bromide functionalized membrane: .....	41
5.1.4 Hydrolysis of PtBA brushes grown TFC PA membrane: .....	42
5.2 Optical Microscopy analysis:.....	43
5.3 FTIR-ATR: .....	44
5.3 Water contact angle analysis: .....	46
5.4 Scanning electron microscopy SEM:.....	48
5.5 Optical profilometry: .....	51
5.6 Permeation flux:.....	52
5.7 Salt rejection: .....	54
5.8 pH responsive behavior of PAA brushes:.....	56
5.9 Mechanical Testing.....	58
Chapter 6: Conclusions.....	61
Chapter 7: References.....	63

# List of figures

Figure 1 Mechanism of membrane separation .....	6
Figure 2 The filtration range of micro, ultra, nano and reverse osmosis membrane.....	7
Figure 3 Schematic of typical membrane process for water treatment. ....	8
Figure 4 RO membrane filament structure. ....	12
Figure 5 Interfacial polymerization reaction of 1,3-phenylene diamine and 1,3,5-trimesoyl chloride. ....	12
Figure 6 General mechanism of ATRP .....	18
Figure 7 Overall equilibrium reaction of ATRP.....	19
Figure 8 A) Grafting to, B) Grafting from, techniques .....	22
Figure 9 Initiator attachment on APTMS functionalized RO membrane.....	26
Figure 10 Growth of polymer brushes.....	27
Figure 11 Purification of copper bromide .....	28
Figure 12 Graphical representation of a single reflection ATR. ....	30
Figure 13 BRUKER, Model ALPHA FTIR-ATR.....	30
Figure 14 SEM schematic .....	32
Figure 15 Signals emitting from different parts of interaction volume.....	33
Figure 16 Working of optical profilometry. ....	36
Figure 17 Nanovea PS-50 optical microscope. ....	36
Figure 18 Optika B-600 optical microscope .....	37
Figure 19 Optical microscopy of a) simple membrane b) TFC PA—NH <sub>2</sub> c) TFC PA---Br d) TFC PA – PtBA brushes. ....	43
Figure 20 FTIR-ATR analysis of a) PA, b) PA-NH <sub>2</sub> , c) PA-Br, d) PA-g-PtBA.....	45
Figure 21 FTIR analysis of TFC PA-PAA.....	45
Figure 22 Contact angle images of TFC-PA (A), PA- NH <sub>2</sub> (B), PA-Br(C), PA-g-PtBA (D) and PA-g-PAA (E) membranes. ....	47
Figure 23 SEM A, B,C and D are surface morphology of PAA-g-PA ,E, F,G and H for simple membrane.....	49
Figure 24 SEM images A, B, C & D cross-section of PAA-g-PA and images E, F, G & H cross-section of simple membrane .....	50



Figure 25 Graph showing the surface roughness values of all samples .....	52
Figure 26 Graph showing the permeation flux for five cycles at pH 3 and 11 .....	53
Figure 27 Graph showing the comparison between the fluxes of neat and modified membrane at pH 3 ,7 and 11.....	54
Figure 28 Graph showing the %salt rejection rate .....	56
Figure 29 Mechanism of protonation and deprotonation of PAA brushes at low and high pH .....	57
Figure 30 Model showing PAA conformation at low and high pH and its effect on flux .....	57
Figure 31 Stress-strain curves of Pristine PA and PAA-g-PA .....	59
Figure 32 Graph showing the ductility of the Pristine PA and PAA-g-PA.....	59

# List of tables

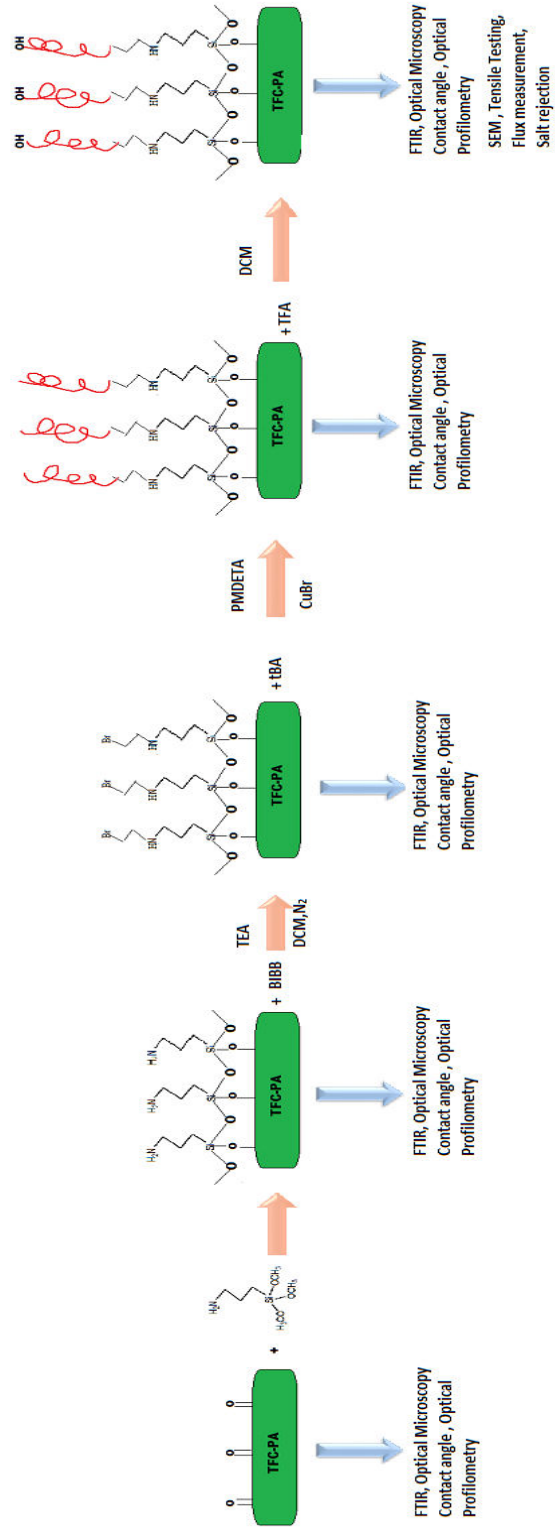
Table 1 Properties of different types of membrane for water treatment .....	11
Table 2 Contact angles of the membrane samples .....	47
Table 3 Surface roughness Ra values of membrane samples.....	51
Table 4 Permeation flux and % salt rejection at pH 3 , 7 and 11 .....	55
Table 5 : Mechanical properties of pristine PA and PAA-g-PA .....	58

# List of Abbreviations

ATRP	Atom transfer radical polymerization
RO	Reverse osmosis
APTMS	3-aminopropyl trimethoxy silane
BIBB	$\alpha$ -bromo isobutyl bromide
FTIR-ATR	Fourier transform infrared spectroscopy-attenuate total reflectance
SEM	Scanning electron microscopy
KPa	Kilo pascal
THM	Trihalomethane
NF	Nanofiltration
PS	Polysulfone
CA	Cellulose acetate
PVDF	Poly vinylidene fluoride
PI	Polyimide
PES	Polyether sulfone
PAN	Poly acrylonitrile
TFC	Thin film composite
PA	Polyamide
MMM	Mixed matrix membrane
CNT	Carbon nanotubes
TFL	Thin film composite
MF	Microfiltration
UF	Ultrafiltration
PVA	Polyvinyl alcohol
TMMAM	Trimesoylamido amine
SWNT	Single walled carbon nanotubes
UV	Ultraviolet
IUPAC	International union of applied chemistry
PtBA	Poly tertiary butyl acrylate

PAA	Poly acrylic acid
DCM	Di-chloro methane
°C	Degree Celsius
PMDETA	N, N, N', N'', N''' Penta-methyl diethylene triamine
THF	Tetra hydrofuran
TFA	Trifluoro acetic acid
CCD	Charged coupled device

# Surface Modification of TFC-PA RO membrane by grafting hydrophilic PAA polymer brushes through ATRP



# Chapter 1: Introduction

## 1.1 Background:

Water, which has chemical formula of H<sub>2</sub>O, two hydrogen atoms attached to one oxygen atom makes up one molecule of water. Water is the most abundant natural resource available to human beings. But nowadays, it is the most unavailable to most population in the world. Most countries in Africa and Asia has been facing the shortage of fresh water [1]. Fresh water scarcity is one of the largest concerns facing by modern society. The “fresh water” can be defined as the water with less than 500ppm to 1000ppm of dissolved salt [2]. The earth where we live comprises of 71% of water and remaining 29% is land. In 71% water, available only 2.5% of total can be used by humans and rest of it is not fit for human use. But only 0.01% is clean and fresh water. Per UNO, the fresh water is basic human right and other creature but still it is unavailable to approximately 2.8 billion people on the earth [3]. By 2025 this number is projected around 3.5 billion. As the world population is increasing day by day, the availability of fresh water is becoming scarce.

## 1.2 Water pollution in Pakistan:

Among many problem relating to public health, water pollution is one of the major challenges nowadays. Quality of portable water in Pakistan falls well below the acceptable range. Pakistan’s drinking water quality lies 80 among 122 countries [4], [5]. Water present on surface and ground, both are contaminated with toxic metals, pesticides, organic materials etc. The standards set by WHO for portable water are not obliged by organizations in Pakistan. The trend of urbanization and industrialization has a major impact on quality of life, as the standard of living has improved, it has adverse effect on the natural environment especially the water resources. The major water borne diseases like diarrhea, cholera, hepatitis etc. are the major issue caused using unsafe water in Pakistan [6].

### **1.3 Emergence of Polymeric membrane:**

Membrane, a barrier which allows certain things to permit and block the rest. The things may be atoms, ions molecules and small particles. There are different kinds of membranes such as biological membranes, nuclear membranes and synthetic membranes. The concept of membrane technology has been using from eighteenth century. Different life sustaining process which are important make use of membrane technology. Polymeric membranes are widely use in water treatment due its low cast and ease with its fabrication [7]. One of the major concern for membrane based water treatment is fouling which is initially natural concentration polarization during filtration [8]. Permeate quality and permeation rate-over the time can be adversely affected by fouling [9]. Membrane fouling is major concern and efforts have been undergone to control the membrane fouling.

### **1.4 Membrane fouling:**

Despite of low cost, polymer membrane has several disadvantages. Among them membrane fouling is a core issue. Fouling occur due to unwanted interaction between membrane surface and foulant molecules. Membrane surface morphology such as surface roughness and charge, surface roughness and charge, surface hydrophilicity/hydrophobicity and the nature of the foulant molecules to be attached onto the membrane surface will greatly influence the membrane fouling [10]. The membrane surface with a high degree of roughness tend to have high fouling rate than the smooth surface [11]. The more the hydrophilic surface, less likely to be fouled [12]. As the hydrophilicity increases, the more it attracts the water molecule towards itself and prevent the membrane surface from the attack of foulant due to hydrophilic-hydrophobic repulsion. Negatively charged surface may form fouling through the interaction with the positively charged foulant molecules [13]. Membrane fouling could be reversible, irreversible depending upon the state of foulant attached to the membrane surface [14]. Often simple hydraulic cleaning is

employed for the cleaning of reversible fouling which mainly occur due to the reversible adsorption of foulant [15]. On the other hand, irreversible fouling occurs due to the strong physio-sorption and/or chemisorption of foulant molecules on the membrane surface and in pores [16]. Chemical and/or thermal treatment is often required for irreversible fouling, which results in decline of membrane life [17]. Various physical and chemical techniques have been proposed to modify the membrane surface to reduce the membrane fouling and to enhance the membrane performance.



## 1.5 Research framework:

### PHASE I

Synthesis of Poly t-butyl acrylate by the ATRP. Formation of green colored viscous liquid indicates the formation of polymer.

### PHASE II

Surface modification of RO membrane which took place in three steps

- 1) Attachment of amine ( $--NH_2$ ) on the surface of membrane by the reaction of APTMS with the membrane. The modified membrane is characterized using FTIR-ATR, Optical microscopy, optical profilometry and contact angle measurement.
- 2) Bromination of amine attached membrane by the reaction of BIBB which act an initiator for growth of polymer brushes with the membrane. The modified membrane is characterized using FTIR-ATR, optical microscopy, optical profilometry and contact angle measurement.
- 3) Initiator attached polymer are reacted with the t-butyl acrylate for the growth of polymer brushes. The modified membrane is characterized using FTIR-ATR, optical microscopy, optical profilometry and contact angle measurement.

### PHASE III

The polymer brushes grown membrane is characterized using SEM. After the SEM analysis, the modified membrane is then hydrolyzed. After that the flux permeation is measured that of modified membrane.

## **1.6 Aims and objectives:**

Following are the main aims and objectives of research work

- Synthesis and characterization of poly t-butyl acrylate
- Surface modification of RO membrane with polymer brushes
- Characterization of modified membrane
- Aim of fabrication of modified membrane is to increase
  1. Permeability flux
  2. Hydrophilicity

# Chapter 2: Literature Review

## 2.1 Membrane technology:

### 2.1.1 What is membrane technology:

A membrane is a selective barrier that permits the separation of certain species in a fluid by combination of sieving and diffusion mechanisms [18]. Membranes can separate particles and molecules and over a wide particle size range and molecular weights.

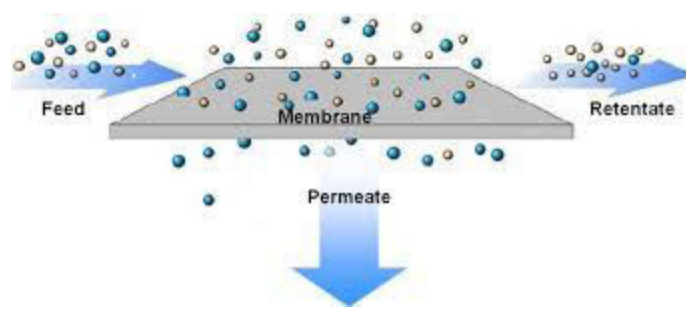


Figure 1 Mechanism of membrane separation

## 2.2 Types of membrane separation processes:

Membrane separation process is categorized in three way

1. Pressure driven membrane
2. Electrically driven membrane process
3. Novel Membrane process

### 2.2.1 Pressure driven membrane processes:

Pressure driven processes use hydraulic pressure to force water molecules through the membrane. The impurities are retained in the feed stream and clean water is retrieved on the either side of the membrane [19]. Pressure driven membranes are further classified as

1. Microfiltration

2. Ultrafiltration
3. Nanofiltration
4. Reverse osmosis

The filtration ranges and type of contaminants which they could clean is given in the form of figure 2

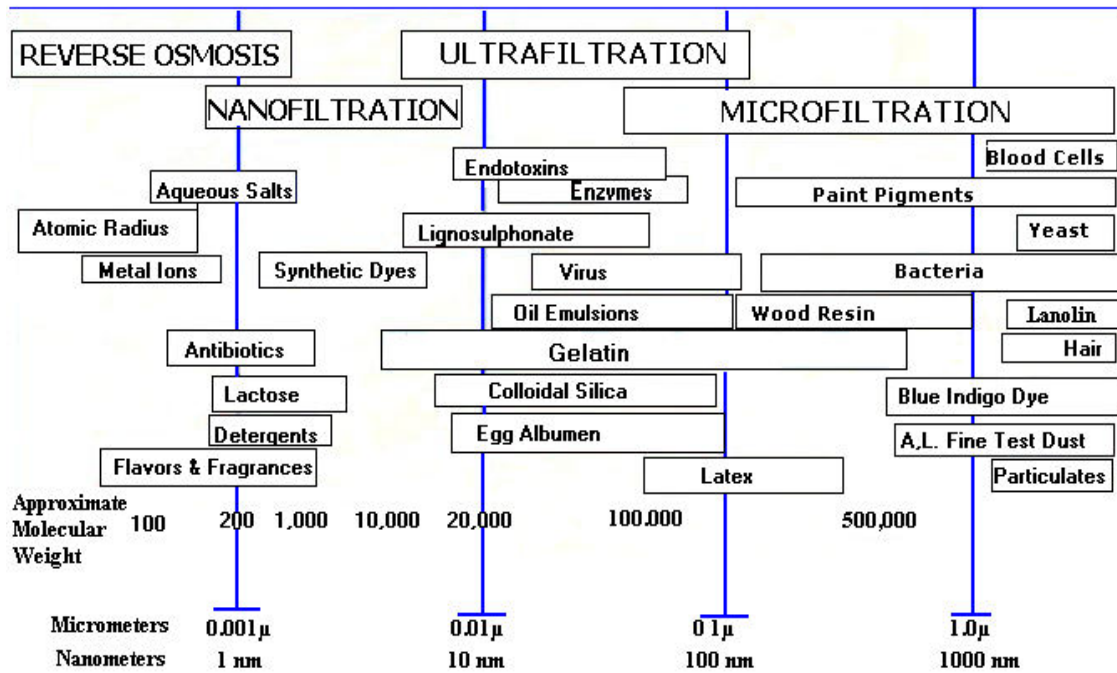


Figure 2 The filtration range of micro, ultra, nano and reverse osmosis membrane

### 2.2.2 Electrically driven membrane processes:

In electrically driven membrane process, the ions are forced to move through the membrane using electric current. In this case the clean water remain at the feed stream [20].

The electrically driven membranes are classified as

1. Electro dialysis
2. Electro deionization

### 3. Capacitive deionization

#### 2.2.3 Novel membrane processes:

Novel membrane processes are also termed as osmotically driven membrane system. These system uses almost negligible pressure to pump fluid across the membrane. Novel membrane process includes

1. Membrane distillation
2. Forward osmosis membrane

#### 2.3 Membrane technology for water treatment:

The membrane technology which are used commercially for water treatment nowadays is pressure driven membranes where the driving force is the pressure difference across the membrane [19]. These membrane processes are used for the treatment of water in which the clean water is separated in the form of stream called as filtrate or permeate and the remaining contaminants are termed as concentrates.

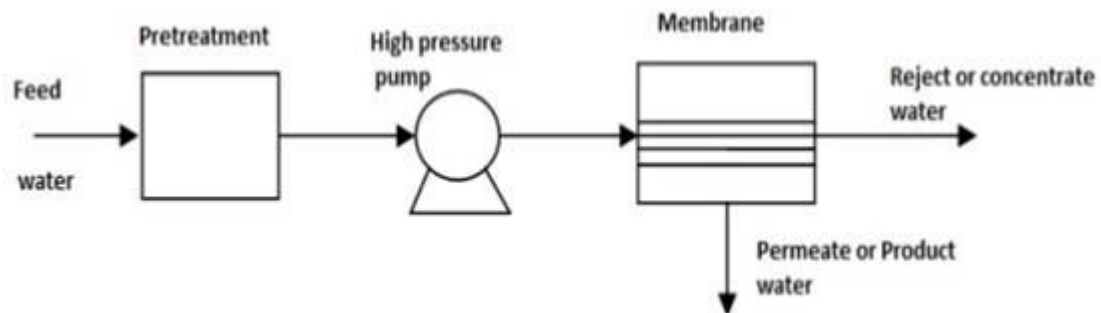


Figure 3 Schematic of typical membrane process for water treatment.

The membrane used in the treatment process is an excellent barrier. This system allows continuous and reproducible filtrate or permeate quality. Along with the high quality of permeate, membrane process is independent of type of contaminant in the feed. Membrane used for water treatment can be classified as

1. Microfiltration
2. Ultrafiltration

3. Nano-filtration
4. Reverse osmosis

The classification of the membrane is based on the capabilities of the process which are discussed in following section.

### **2.3.1 Microfiltration:**

Microfiltration is the least constraining membrane type. It is employed for the removal of submicron contaminants or particles such as bacteria, emulsion particles etc. The pore size of these membranes is in the range of ca. 1-10 $\mu$ m. Mostly these commercial membranes have average pore size of 0.2 $\mu$ m. These need an operating pressure of 500 KPa (5bar) [21].

### **2.3.2 Ultrafiltration:**

Ultrafiltration membranes are used for removal of bacteria and viruses. It can also be used for the separation of macromolecules such as sugar and proteins, also colloidal silica and pyrogens [22]. Ultrafiltration membrane has a typical pore size of 0.05 $\mu$ m and operate at a pressure of 1000 KPa (10bar) [23].

### **2.3.3 Nanofiltration:**

The Nanofiltration membrane operate on the principle of solution diffusion. In solution diffusion, the monovalent ions diffuse through the membrane. Colour removal, sugar and dye removal can be done by nanofiltration [24]. It can also be used for removing THM precursor and sulfate in the wastewater supplies. NF has typically pore size of 1 to 5nm and 5000kPa(50bar) pressure is needed for filtration [25].

### **2.3.4 Reverse Osmosis membrane:**

Reverse osmosis membrane is most dense type of membrane commercially available. It also works on the principle of solution diffusion. Dissolved salts and ions having molecular weight less than 200g/mol are usually separated by using reverse osmosis membrane[26]. It is used to produce ultrapure water for the use in pharmaceutical and semiconductor. The pressure range for the operation of reverse osmosis system is in the range of 7000 kPa (70bar) to 15000 kPa (150bar) [27][28].

Properties of above described membrane processes can be summarizing in the form of table

<b>Feature</b>	<b>Microfiltration</b>	<b>Ultrafiltration</b>	<b>Nanofiltration</b>	<b>Reverse Osmosis</b>
Polymers	Ceramics, sintered metals, polypropylene, polysulfone, polyethersulfone, polyvinylidene fluoride, polytetrafluoroethylene	Ceramics, sintered metals, cellulosics, polysulfone, polyethersulfone, polyvinylidene fluoride	Thin film composites, cellulosics	Thin film composites, cellulosics
Pore Size Range (micrometers)	0.01 - 1.0	0.001 - 0.01	0.0001 - 0.001	<0.0001
Molecular Weight Cutoff Range (Daltons)	>100,000	2,000 - 100,000	300 - 1,000	100 – 200
Operating Pressure Range	<30	20 – 100	50 - 300	225 - 1,000
Suspended Solids	Yes	Yes	Yes	Yes

Removal				
Dissolved Organics Removal	None	Yes	Yes	Yes
Dissolved Inorganics Removal	None	None	20-85%	95-99%
Microorganism Removal	Protozoan cysts, algae, bacteria	Protozoan cysts, algae, bacteria	All	All
Osmotic Pressure Effects	None	Slight	Moderate	High
Concentration Capabilities	High	High	Moderate	Moderate
Permeate Purity	High	High	Moderate-high	High
Energy Usage	Low	Low	Low-moderate	Moderate
Membrane Stability	High	High	Moderate	Moderate

Table 1 Properties of different types of membrane for water treatment

Reverse osmosis membrane filament has three parts. First is the active layer of TFC polyamide, second is the PES support layer and third is the nonwoven polyester fabric as shown in figure.



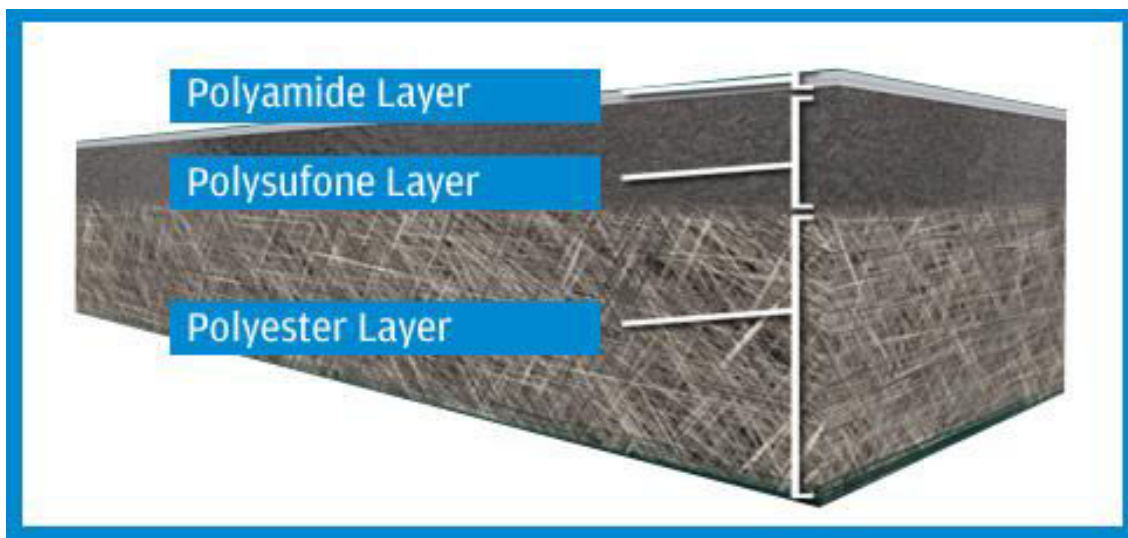


Figure 4 RO membrane filament structure.

Number of RO membrane materials can be employed for water desalination, but not all of them can produce desired result. The membrane materials which are commercially used for this purpose are polysulfone (PS) [29][30], cellulose acetate (CA) [31]–[33], polyvinylidene fluoride (PVDF) [34]–[36], polyimide (PI) [37], [38], polyether sulfone (PES) [39]–[41] and polyacrylonitrile (PAN) [42]–[44].

## 2.4 Thin film composite polyamide membrane:

Polyamides are the polymers in which repeating units are amides. The amides have -CO-NH-, linkages. Naturally occurring polyamides are the proteins. TFC polyamides have been produced from the interfacial polymerization reaction of 1, 3- phenylene diamine and 1,3,5-trimesoyl chloride.

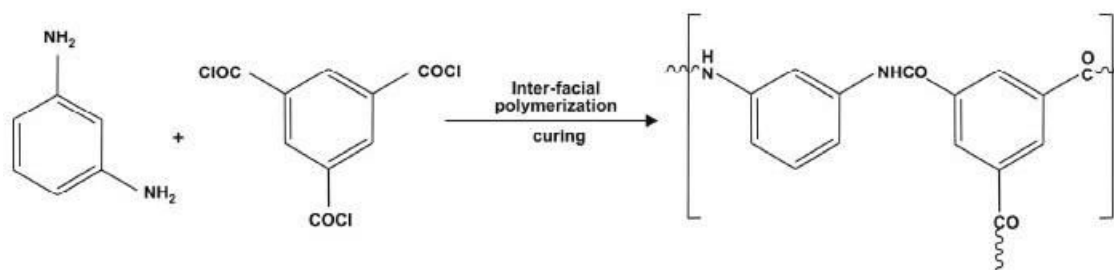


Figure 5 Interfacial polymerization reaction of 1,3-phenylene diamine and 1,3,5-trimesoyl chloride.

TFC polyamide membrane are aromatic membranes with high chemical and mechanical resistance [45]. They have excellent performance in the field of desalination and water purification technologies. Typically, they have a pore size of 200nm.

Contact angle analysis is one of the widely-used technique used to study the membrane hydrophilicity/hydrophobicity. Main factors that influence the contact angle values are porosity, roughness and pore size distribution. Hydrophilicity is directly related to contact angle, if the contact angle of water drop with the membrane surface is large, it means that membrane has high hydrophilicity index. If the pore size is large than the contact angle would be small. Also, the contact angle value declines with the decrease in surface roughness of membrane [46].

Hydrophilicity has great effect on the fouling of membrane. Fouling can be decreased by increasing the hydrophilic character of the membrane. By increasing the hydrophilicity, water molecules can easily be attracted towards the membrane. Due to hydrogen bonding ability of water, the water molecule attached to membrane surface help other water molecules to adhere to the membrane. Once the bonding is established it cannot be easily break [46].

Control of membrane structure is needed to enhance the performance of membrane. It is difficult to control the structure of membrane. Several factors such as type of polymer, the solvent and solvent type and concentration, temperature and composition coagulation bath governs the performance and the structure of membrane. Other way to increase the membrane performance is to functionalize the membrane surface which can be achieve by coating, self-assembly, plasma treatment and chemical grafting [47].

## **2.5 Methods for the modification of PA membrane:**

There are many ways for the modification of PA membranes. They are fall into three main approaches [48]

- 1) Bulk modification of PA material and then to prepare modified membranes.
- 2) Surface modification of prepared membrane
- 3) Blending, which can also be regarded as surface modification

In fact many kinds of methods are used for the modification of PA membranes such as physical methods which includes blending and surface coating methods [49]–[51], chemical methods including photo-induced grafting [52], gamma ray [53] and electron beam induced grafting [54], plasma treatment and plasma induced grafting [55]–[57], thermal induced grafting and immobilization [58], [59], surface initiated atom transfer radical polymerization [58], [59] and so on.

Brief overview of some of the modification techniques are as follow

### **2.5.1 Bulk modification:**

Bulk modification is done by reacting the desired functional group reagent with the membrane material. After the completion of reaction, the material formed is used for the fabrication of membranes. One of such modification is done by the reaction aqueous isopropyl alcohol with the TFC PA membrane. It is a short span chemical reaction which helps in the limited hydrolysis and fluorination with the improved antifouling properties [60].

### **2.5.2 Blending methods:**

It is the simplest and most widely used technique for the modification of TFC-PA membrane. It can be used for both flat sheet and hollow fiber but the result are no seem to be remarkable. Commercial cellulose acetate and polyamide RO membrane can be modified using a homologous series of polyethylene-oxide surfactant [61]. By blending them with PA the membrane can be easily modified. They can enhance the properties such as hydrophilicity and antifouling but the leaching of these polymer may occur. Now amphiphilic copolymers are synthesized and can be used for blended with PA [62]. Other than polymeric organic materials, inorganic materials have been using for blending purpose. One such example is mixed matrix membrane (MMM) in which zeolite loading is used to enhance the properties [63]. Recent studies show that different type of nanoparticles blended with PA membrane. One such study is the blending Titania (TiO<sub>2</sub>) nano particles with PA membrane shows the enhancement of antifouling properties [64]. Studies also shown the use CNT's and graphene for this purpose [65], [66].

### **2.5.3 Surface-coating TFC-PA membrane:**

In a surface coating method, TFC-PA membrane is coated by directly depositing a selective thin layer forming a thin film layer (TFL). Mostly this technique can be used for the conversion of MF/UF membrane into NF membrane [48]. One of such example of this type of modification is the coating of TFC-PA membrane with polyvinyl alcohol (PVA) then crosslinking it which results in the enhancement of antifouling properties and hydrophilicity [67]. A self-made dendritic molecule of TMMAM has been coated over TFC polyamide RO membrane to improve the water flux without the salt rejection antifouling and chlorine tolerant properties [68].

### **2.5.4 Surface coating via interfacial polymerization:**

There is no reaction to occur during the simple coating method whereas a chemical reaction occurs at the interfacial boundary of two immiscible solutions during the interfacial polymerization. Usually a reaction occurs when a water-soluble monomer and an organic soluble monomer are brought together at the interface between water and water immiscible organic solvent. The polymer can be easily coated on the PA membrane and this polymerization occurs on the membrane surface and pore surface during the interfacial polymerization. Since a chemical reaction is involved during surface coating so it can be used only on flat sheet membrane, hollow fiber membranes are difficult to modify by this process [48]. One of such example is the interfacial polymerization of polyamide-aluminosilicate SWNT nanocomposite membrane which results in the higher rejection rate of divalent ions as compared to monovalent ion [69].

### **2.5.5 Photo-induced grafting PA membrane:**

This photochemical technique is an attractive one for the modification TFC-PA membrane. It has several advantages such mild reaction conditions and ambient temperature, high selectivity of monomer and respective wavelength. This technique is mainly used for the modification of flat sheet membrane whereas hollow fiber membrane is difficult to modify by this process. Mostly photoactive monomer is used for the modification. There are many publications about the UV irradiated induced

grafting of vinyl monomers on the surface of polyolefins. Polyethylene glycol has been grafted on the polyamide membrane which results in the increase in the hydrophilicity, permeate flux and the antifouling properties [70].

#### **2.5.6 Gamma ray and electron/ion beam-induced grafting TFC-PA membranes:**

This technique uses the gamma rays to start the modification. High energy of intense gamma ray led to the formation of free radical by the induced chemical bond breakage. The radical formed will initiate the polymerization process compared to the conventional method in which the initiator is needed to start the polymerization process. As we know gamma rays are very high energy beams which is used for bond breaking, it would affect the strength of membrane, so this method is seldom used.

Ion beam irradiation is an alternative method of induced grafting. By this technique an active site is created with the help of an ion beam, allowing the monomer to be attached on the active surface of the membrane. This method is used for the formation of anionic and cationic membranes. The attachment of 1-vinylimidazole on the surface of TFC RO membrane with the help of gamma ray irradiation has improved fouling and flux properties [71].

#### **2.5.7 Plasma treatment and plasma-induced grafting polymerization:**

Many plasma treatments have been introduced to make the permanent hydrophilic membrane surface. Plasma can be generated by ionization of gas and water which is used for the modification of membrane. Plasma treatment can also be used for the formation of active site on the membrane surface for the grafting purposes. Radio waves and microwaves are often employed for the ionization of gas by mean of electric discharge at a very high frequency. The upper layer of the membrane surface is activated with the help of plasma components to increase the hydrophilicity without affecting the bulk polymer [72]. Plasma treatment can be used for the introduction of variety of functional groups on the membrane surface by varying the conditions. The use of gas in plasma treatment depends upon the host material. Low pressure plasma helps in the enrichment of amine group on the TFC RO membrane used for antimicrobial properties [73]. In another experiment a single step plasma

polymerization process is used to deposit hydrophilic polymer triglyme on the surface of TFC RO membrane for low organic fouling [74].

#### **2.5.8 Thermal induced grafting and immobilization:**

PES membrane can be superficially modified by using this technique. In this method, a chemical initiator or cleavage agent is needed. A simple chemical procedure is needed to covalently immobilize the TFC RO membrane surface for the attachment of biomolecule such as enzyme, protein, amino acids [75]. One such work is done by Shi and Jiang et al, they prepared the antifouling and self-cleaning membrane surface. They have achieved this by covalently attachment of trypsin on poly (methacrylic acid)-graft-polyether sulfone (PMMA-g-PES) membrane [76].

#### **2.5.9 Initiated chemical vapour deposition method:**

It is an all-dry free radical polymerization technique which has been carried out at low temperature and low operating pressure. By this technique yang et al, has synthesized a copolymer containing poly-sulfobetain zwitteric ion group which has been covalently bonded to RO membrane [77]. In this method modifier is chemically attached to membrane surface.

#### **2.5.9 Surface Initiated ATRP:**

Atom transfer radical polymerization the most convenient and one of the successful method of grafting new synthesized polymer on the membrane surface. The reason is that this technique promises to carry out at mild conditions and variety of vinyl monomer can be polymerized in a controlled way and well defined structures can be achieved [78].Zhang et al. has grafted poly sulfobetain methacrylate on the polyamide surface through ATRP to improve the fouling properties of TFC RO membrane [79]. Until now there are grafting strategies of ATRP for the membrane modification namely, grafting through, grafting from and grafting to. Detailed description of ATRP will be carried out in next section.

### **2.6 Atomic transfer radical polymerization ATRP:**

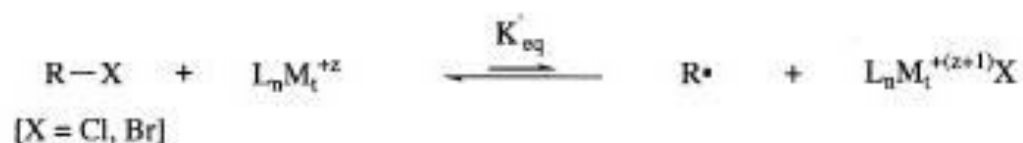
According to IUPAC the ATRP is defined as “It the type of controlled reversible-deactivation radical polymerization in which the deactivation of the radicals involves reversible atom transfer or reversible group transfer catalyzed usually though not exclusively by transition metal complexes.”

In the reaction where the ATRP occurs, atom transfer is the main step used for the uniform polymer chain growth. Mitsuo Sawamoto and by Jin-Shan wang and Krzysztof Matyjaszewski in 1995 has discovered the ATRP.

### 2.6.1 General mechanism of ATRP:

Typical ATRP is represented by following mechanism [80]

Initiation:



Propagation:



Termination:

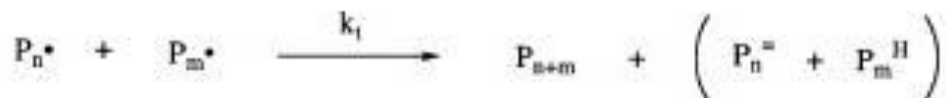


Figure 6 General mechanism of ATRP

The overall equilibrium of ATRP is given as

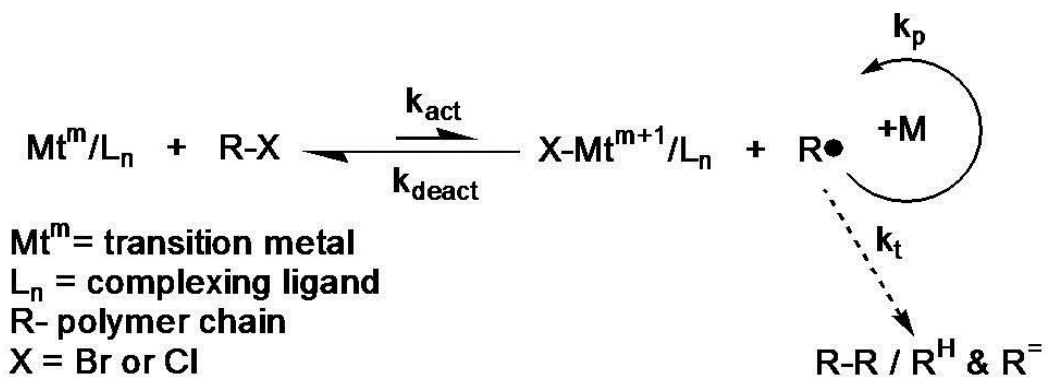


Figure 7 Overall equilibrium reaction of ATRP

Alkyl halide is used as an initiator (R-X) and transition metal complex as catalyst during ATRP. The catalyst used during ATRP are mainly Cu, Fe, Ru, Ni, Os [80], [81]etc. The activation of dormant species is carried out by the transition metal catalyst through an electron transfer process to generate a free radical. During this process the catalyst is oxidized to higher oxidation state. It is the reversible process which rapidly establishes an equilibrium and the equilibrium is mainly shifted toward very low concentration side. The number of polymer chain depends upon the number of initiators. In ATRP each polymer growing chain has equal opportunity to propagate with monomer to form living polymer chains (R-P<sub>n</sub>-X). This results in the formation of polymer chain with similar molecular weight and narrow molecular weight distribution.

ATRP has many advantages over conventional polymerization as it a robust technique. It can make use of many functional groups such as amino, allyl, epoxy, vinyl and hydroxy group. Ease of preparation, commercially available and inexpensive catalysts, pyridine based ligands and initiators make it a diversified technique [81], [82].

### 2.6.2 Components of normal ATRP:

There are four important variable components of ATRP which are namely monomer, initiator, catalyst and solvents.

#### 2.6.2.1 Monomers:

In ATRP, the monomer which are used usually have the substituents so that it can stabilize the propagating radicals e.g. styrene, (meth)acrylates, (meth)acrylamides and



acrylonitrile.[80] If the concentration of the propagating radical balances the rate of radical termination, the polymer will have high molecular weight with low polydispersity index. So, for good polymerization other components of polymerization must be synchronized with the concentration of dormant species as it should be equal or higher than the propagating radical [81].

#### 2.6.2.2 Initiator:

Initiator is the main component which controls the number of growing chains. Rapid initiation results in the polymer of narrow weight distribution and the consistency of number of propagating chains [81]. Alkyl halides are the commonly used initiator during the process as they are similar to organic framework as the propagating radical [83]. Among the alkyl halide mostly alkyl bromides are used as they are more reactive than alkyl chlorides but both have good control of molecular weight [81]. The architecture of polymer is governed by the shape and structure of initiator [84].

#### 2.6.2.3 Catalyst:

The most important component of ATRP is the catalyst. Equilibrium constant between the dormant and active species depends upon the catalyst. Equilibrium constant determines the polymerization rate. If the equilibrium constant is small then the rate of polymerization is low and if the equilibrium constant is too high then there will be high distribution of chain lengths [81].

There are some requirements for the metal catalyst to be used in ATRP.

- a) There needs to be two accessible oxidation states that are separated by one electron
- b) The metal center should have high affinity for halogen
- c) The coordination sphere of the metal will be able to accommodate halogen when it is subjected to oxidation.
- d) Transition metal catalyst should be inert so it cannot give side reactions such as reversible coupling with the propagating radicals and catalyst radical termination, etc.

According to most of the studies copper is among those which met the criteria having versatility with wide range of monomers [85].

#### 2.6.2.4 Solvents:

The solvents which are most likely to be used are toluene, 1,4-dioxane, xylene, anisole, DMF, DMSO, water, methanol, acetonitrile and DMC,[86] etc.

### **2.7 Polymer brushes:**

Polymer brushes are the long chain polymer molecules attached to the one end by the surface or interface with the density of attachment so high that the chains are forced to stretch away from the interface [87].

The reason behind the use of polymer brushes for the modification of membrane is due to its colloidal stabilization, modification of bulk surfaces and interface to improve adhesion, wetting and wear properties. The interface used may be solid interface, interface between two solvents, between solvent and air [87].

There are two methods of producing polymer brushes namely physical and chemical processes.

Physical process refers to coating of surface without any covalent bonding and there is always a chance of desorption. Only the electrostatic and Vander Waal's attraction exist [88].

Chemical process involves the formation of covalent between the surface and coating. There are two types of chemisorption process namely grafting to and grafting from.

The grafting to approach involves already prepared end functionalized polymer with suitable moieties exposed onto the surface. The main drawback of this method is the inherent diffusion limitation affecting the grafting reaction [89].

The grafting from approach the surface to be modified is activated by attaching a suitable initiating species, then the growth of polymer chain takes place. The initiating specie comprise the molecules which could carry out polymerization by ATRP [89].

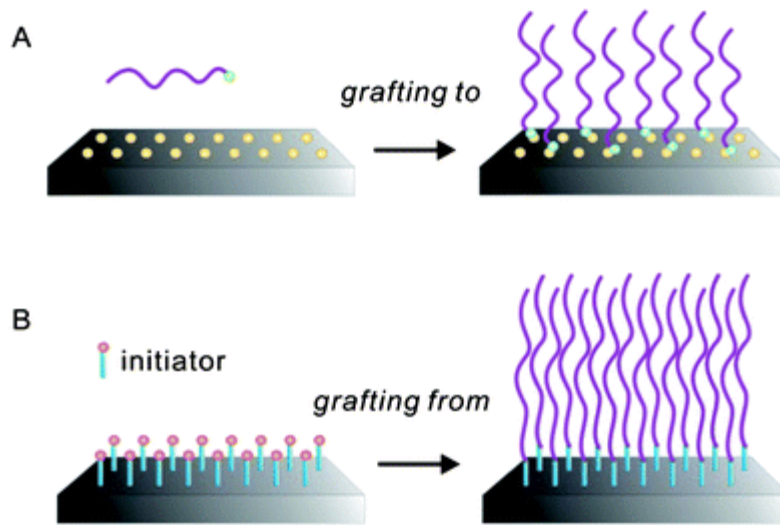


Figure 8 A) Grafting to, B) Grafting from, techniques

This study is about the growth of polymer brushes by ATRP in which grafting from approach is used.

### 2.7.1 Why to choose ATRP for polymer brushes:

The main reasons for the growth of polymer brushes by ATRP are

- Accurate control of the thickness of polymer layer on the nanometer scale has great importance in the application for chemical separation, sensor and composite material [90].
- Due to ATRP the thickness of polymer brushes can be controlled. low MW polymer can be formed due to the low molecular weight distribution [91].
- The choice of wide variety of monomer make it a versatile technique. Block polymer can be formed thus tailoring the properties of polymer brushes over the wide range [91].
- ATRP can be performed at relative low temperature and this process is easy to execute [92].

### 2.7.2 Controlled synthesis of polymer brushes by ATRP (SI-ATRP):

It is the two-step process

- Immobilization of initiator on the substrate surface

\*the substrate in focus in this current study is TFC-PA membrane

- Atomic transfer radical polymerization.

### **2.7.3 Applications of polymer brushes:**

Polymer brushes has several applications in the field of membrane separation such as

- Protein adsorption and separation [93]
- Solution diffusion separations such as water purification [94], [95]
- Pervaporation of organic compounds [96]
- Gas separation [97]

Polymer brushes can also be used for the stimuli response material [98].

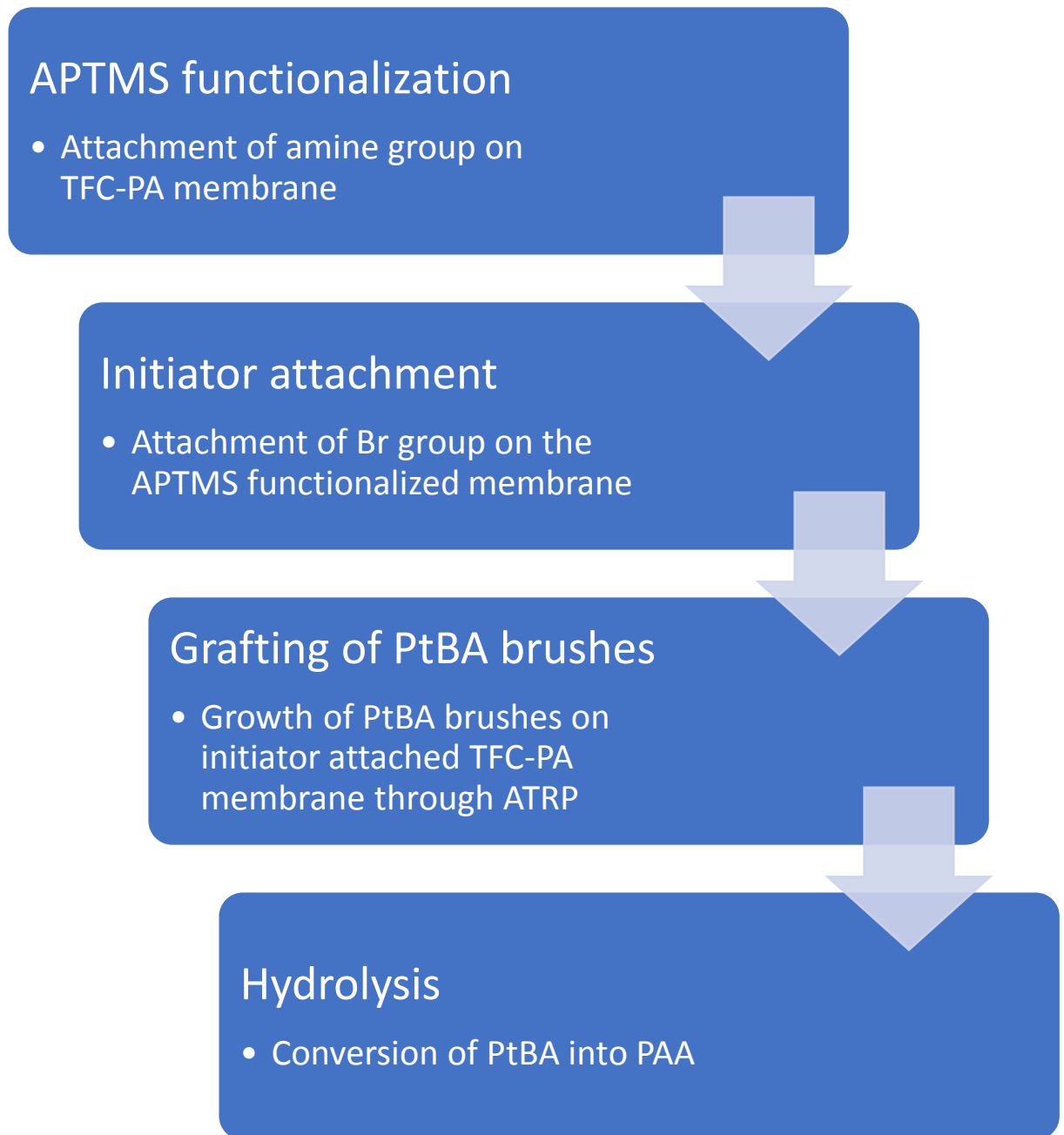
# Chapter 3: Materials and Experimental Work

## 3.1 Materials:

All the chemical used for this experimental work were of analytical grades. This experimental work consists of four steps. For first step, which is functionalization of TFC PA membrane with amine group. We need 3 -Aminopropyl tri-methoxy silane (97%), Distilled water. For second step, which is Functionalization of TFC PA-NH<sub>2</sub> with Br, we need  $\alpha$ -Bromo isobutyl bromide (98%) (initiator), Tri ethylamine (99.5%), Dichloromethane was purchased from Scharlau, Nitrogen gas. Third step is the growth of polymer brushes on the initiator attached TFC PA membrane, we need Copper I bromide (CuBr, 98%), PMDETA (N, N, N', N'', N'''- Pentamethyl diethylenetriamine) (99%), t-butyl acrylate (tBA, 98%), Tetrahydrofuran (99.9%). Fourth step which is the hydrolysis , we need Trifluoro acetic acid TFA were purchased from Scharlau. Glacial acetic acid for the purification of CuBr.

## 3.2 Experimental work:

This experiment is about the modification of TFC PA membrane with t-butyl acrylate polymer brushes.



This experiment consists of four phases

### **3.2.1: Functionalization of TFC RO membrane with APTMS:**

For the functionalization of PA membrane, TFC RO membrane was cut into dimension of 2 inch<sup>2</sup> into four pieces. 60 ml Distilled water was taken in a cultural bottle of 100ml and 4-5 drops of APTMS were added. Then the piece of membrane was put into the

solution and sealed the bottle and left for an hour. After an hour, the membranes were removed and dried under the vacuum at room temperature for 5 hours.

After the membrane was dried, it was cut into four pieces. One part is analyzed by optical microscope, contact angle, optical profilometry and FTIR-ATR. The other three parts are saved for further steps.

### **3.2.2 Initiator attachment on APTMS functionalized TFC RO membranes:**

A solution of 0.37 ml (3mmol, 0.05M)  $\alpha$ -Bromo isobutyl bromide, and 0.41 ml (3mmol, 0.05M) TEA in 60ml of dry DCM was injected over APTMS substrate under the  $N_2$  at room temperature over membranes in a round bottom flask with a continuous stirring for 1 hr as shown in figure 8. After an hour membranes were removed and washed with DCM and absolute alcohol, then dried under the vacuum at 60°C for 1 hr to obtain the initiator functionalized samples.



Figure 9 Initiator attachment on APTMS functionalized RO membrane

One piece of sample is analyzed for contact angle, optical profilometry, optical microscopy and FTIR-ATR. The other two samples were saved for further reaction.

### **3.2.3 Polymer brushes grafting (preparation of TFC PA-tBA membranes):**

60mg of PMDETA, 5 ml of t-butyl acrylate which act as a monomer, 90mg of CuBr were added in the 10 ml glass vial containing membranes placed in a preheated water bath at 60°C and stirred for 4 hrs at 300rpm on hot plate as shown in figure 9.



Figure 10 Growth of polymer brushes

Then membranes were washed with THF and dried under vacuum at 40°C for 4 hrs.

One membrane piece is analyzed for contact angle, FTIR, optical microscopy and optical profilometry. The other part of membrane is saved for next step.

The auxiliary step before this step is the purification of a catalyst as CuBr oxidizes in air. So, it sometime needs for the purification of CuBr.

The purification of CuBr can be done as

Purification of CuBr was done by the Keller-Wycoff method: washing (stirring in round bottom flask) with glacial acetic acid overnight at 300 rpm as shown in figure 11, then filtering it, after that washing two times with ethanol and then drying in vacuum oven at 40°C for 1 hour. Cu(I)Br is almost white (light green) powder





Figure 11 Purification of copper bromide

### **3.2.4 Hydrolysis of polymer brush grafted membrane:**

After the grafting of PtBA on the TFC RO membrane, it was subjected to hydrolysis. 40 ml of DMC was taken in the bottle and 1.5 ml TFA was added and membranes were placed in bottle for 10 mins. The membranes were washed with dichloromethane and dried under the vacuum at 40°C for 4hrs.

# Chapter 4: Characterization techniques

Different characterization techniques which are used to characterize the polymer brushes on the RO membrane are described below.

## **4.1 FTIR-ATR:**

### **4.1.1 Introduction:**

Nowadays, Attenuated Total Reflection (ATR) Is the most widely used sampling tool for FTIR. ATR provides us with the qualitative as well as quantitative analysis of the samples. It requires very little or no sample preparation which greatly speeds sample analysis. The main benefit of ATR sampling is the very thin sampling path length or the depth of the IR beam into the sample. In comparison to traditional FTIR sampling by transmission which requires the dilution of sample with IR transparent salt pressed into pallet or pressed to a thin film, before the analysis to prevent totally absorbing bands in the infrared spectrum.

### **4.1.2 Working of FTIR-ATR:**

Infrared beam into a crystal of relatively high refractive index is used on the ATR sample. The IR beam reflects from the internal surface of the crystal and creates an evanescent wave which projects orthogonally into the sample in intimate contact with the ATR crystal. Some of the energy of the evanescent wave is absorbed by the sample and the reflected radiation is returned to the detector. The phenomena shown graphically for single reflection ATR in figure 12

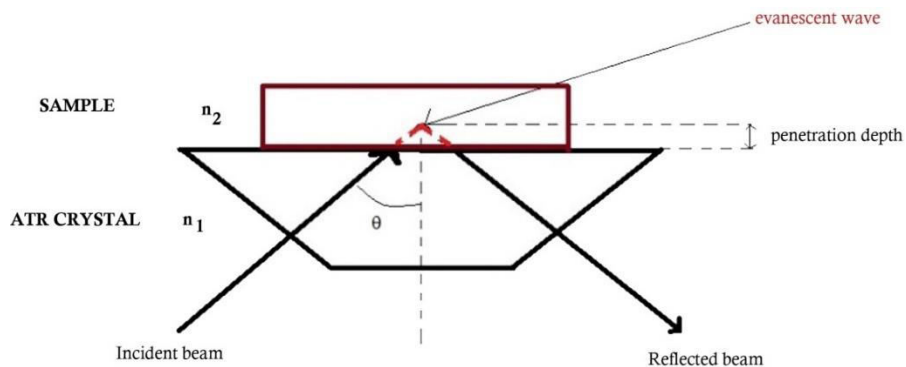


Figure 12 Graphical representation of a single reflection ATR.

#### 4.1.3 FTIR-ATR of membrane samples:

BRUKER's Model ALPHA is used for the confirmation of functionalization of membrane samples.



Figure 13 BRUKER, Model ALPHA FTIR-ATR.

The spectrum is recorded on the computer and analyzed. Five samples, one sample of each step is analyzed using the FTIR-ATR. Each sample has a dimension of  $1 \text{ cm}^2$ .

## 4.2 Scanning electron microscopy: SEM

### 4.2.1 Introduction:

Scanning electron microscopy (SEM), a sophisticated instrument used for the topographical measurement and create images of the sample at a very high resolution. SEM works on the principle of bombarding a beam of electron onto the sample and

analyzing the emitted radiation from the sample. SEM has the resolving power of 1nm and the magnification range is around 5000 to 3,000,00 X.

#### **4.2.2 Construction:**

Generally, SEM is divided into two parts, the electronic console and electronic column. Electronic console division is used for the controls of SEM as it has switches and knobs which are used for the control of filament current, focus, accelerating voltage, magnification, brightness, and contrast.

In an electron column, there is a lens assembly. The electron beam is generated by the filament under vacuum which is accelerated by the help of anodes. The lenses focus the beam onto a small diameter and scanned across the surface of the specimen with the help of electromagnetic coils which also act as lenses. The specimen is placed at the lower chamber of the electron column. Above the sample stage there is a secondary electron detector.

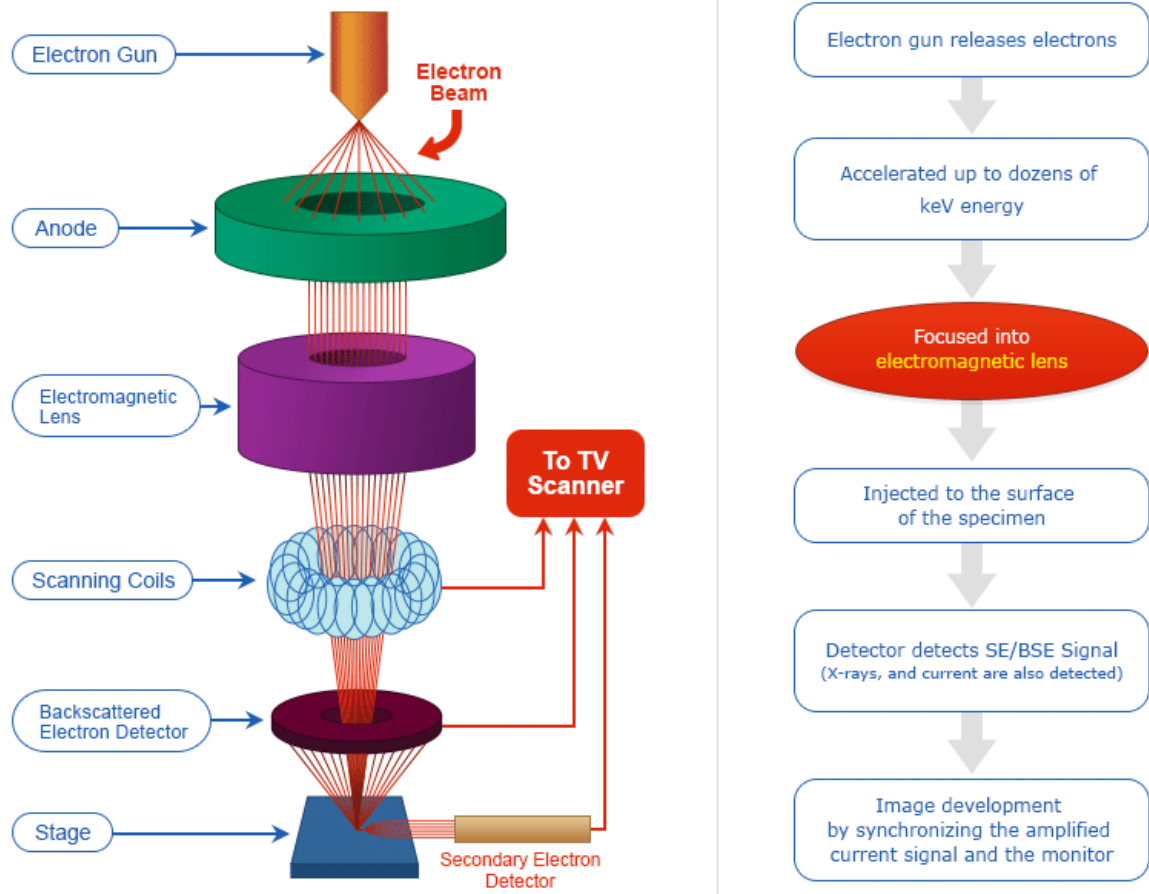


Figure 14 SEM schematic

The conventional optical microscope uses white light as an illuminating source and it has the resolution of the order of 0.2 micron. SEM is used for very high resolution, the maximum resolution which can be achieved by using SEM is 25 Å. As the electron are bombarded on the specimen, it not only gives high resolution but it also generates variety of the signals. These signals give us information about the specimen topography, morphology, chemical nature and structure.

#### 4.2.3 Interaction of electrons with matter:

There are two types of interaction which takes place between specimen and the electrons. Elastic and Inelastic interaction.

During the elastic interaction energy is conserved, only the path of electron changes. During the elastic interaction, back scattered electrons are generated. During the inelastic interaction both path and energy of the electron changes as the energy is transferred to the sample. Secondary electrons are emitted during the inelastic collision.

Normally the electron undergoes multiple interaction and spreading out in a sample with the continuous loss of energy. Due to this the interaction volume within the sample is many times than that of diameter of beam. This penetration results in the variety of signals from the samples including secondary electrons, backscattered electrons and x-rays.

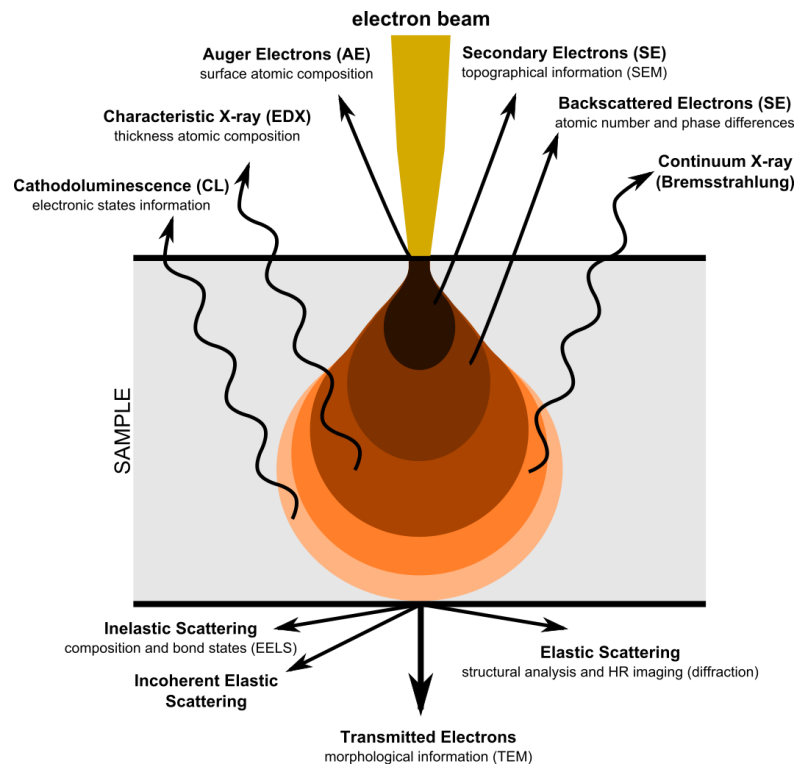


Figure 15 Signals emitting from different parts of interaction volume.

Secondary electrons are generated when the electron beam interact with the loosely bound outer most electron of the sample. Topographical information is given by the electron of low energy (10-50eV). Backscattered electrons are generated by the scattering of SE from the electromagnetic field of nucleus. Secondary electrons are

many times in number than the incoming electrons whereas back scattered electron are few in numbers but have the high energy.

#### **4.2.4 SEM of membrane samples**

Scanning electron microscopy (SEM) model Joel JSM 6490A was used to investigate the morphology, cross section and topography of membrane. Samples are prepared for SEM. Membrane are cut into  $1\text{cm}^2$  pieces, stacked on a steel stud by using carbon tape, gold coated and analyzed.

### **4.3 Contact Angle Analysis:**

#### **4.3.1 Introduction:**

The most important technique for the determination of hydrophilicity is the contact angle measurement. Hydrophilicity will increase with the decrease in the contact angle. Generally, the materials having contact angle less than the 90 degree are generally considering as hydrophilic. So, hydrophilicity or hydrophobicity of the membrane can be determined by contact angle analysis.

#### **4.3.2 Measurement of contact angle:**

Typically contact angle is measured by goniometer. The method employed for measurement is static sessile drop method. In this method, an optical sub method is used to capture a profile of pure liquid onto the solid substrate. The angle formed between the liquid-solid interface and the liquid vapour phase is the contact angle. A high-resolution camera is used to capture the image and then a software is employed to analyze the contact angle.

A  $10\mu\text{l}$  of distilled water is dropped onto the membrane surface. Images are taken through the camera and three different measurements are taken to calculate the contact angle. For the removal of experimental errors by taking the average of the measured values.

## **4.4 Optical profilometry:**

### **4.4.1 Introduction**

Profilometer is an instrument which is used to measure the surface profile to quantify the surface roughness. Dimensions such as step, curvature, flatness are computed from surface topography. This done with the help of probe or light.

There are two types of profilometers. Stylus or contact type is the earliest form of profilometry. Stylus profilometry uses the probe to detect the surface. The probe is typically a hard material such as diamond.

The other type is the optical profilometry or non-contact type which uses light instead of stylus to detect the surface. Optical profilometry is faster than the contact type but with the sacrifice of lateral resolution. The main advantage of optical profilometry is that it does not damage the surface. It can also be used for 3D measurements.

### **4.4.2 Working of optical profilometry:**

In the optical profilometry, a light beam is focused on the sample. After reflecting from the surface the light splits up. As the light splits, constructive and destructive interference takes place forming the light and dark bands, these bands are known as interference fringes. The optical path difference between the fringes depend upon height variance on the sample. The light areas represent the constructive interference whereas dark areas represent the destructive interference. The path difference between the light to dark is one half of the wavelength of the difference between the reference path and the sample path. The point of out of focus means the less interference and high contrast means the best focus.



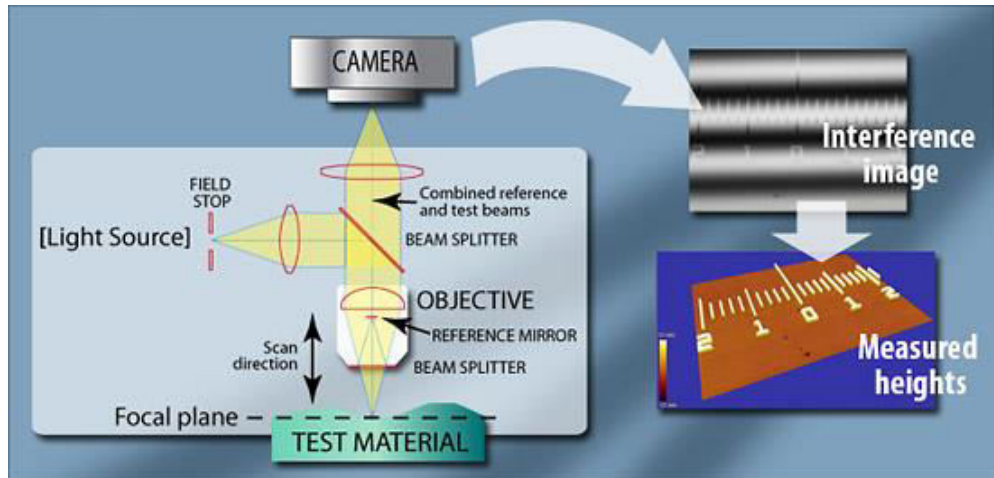


Figure 16 Working of optical profilometry.

#### 4.4.3 Optical profilometry of membrane samples:

NANOVEA PS-50 optical profilometer is employed for the measurement of roughness of membrane samples.

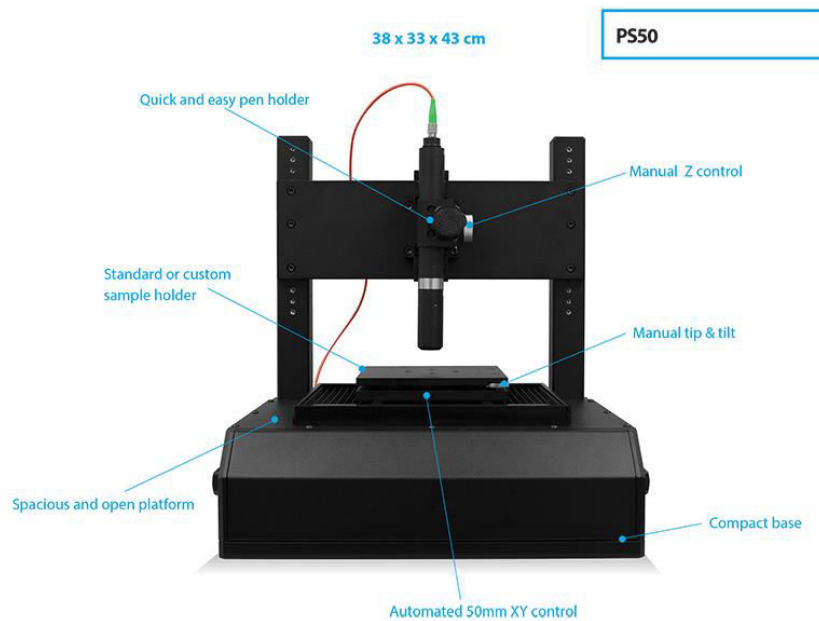


Figure 17 Nanovea PS-50 optical microscope.

The membranes samples are cut into  $1\text{cm}^2$  pieces. Then placed on the plat form. Data is acquitted from the attached computer.

## **4.5 Optical microscopy:**

### **4.5.1 Introduction:**

The other name for the optical microscope is the light microscope as it uses the visible light and the system of lenses to magnify. Basic optical microscopes are very simple, now complex microscopes have been developed to improve the resolution and contrast. Most modern digital microscopes are available with CCD camera to examine the samples showing the results directly on computer rather than seeing through the eye piece.

### **4.5.2 Working:**

The modern optical microscopes are very complex. For accurate measurement, the whole setup of optical path is controlled and accurately set but the working principle is quite simple. The objective is the high magnifying glass lens i.e. of short focal length. The specimen is brought very close to the objective lens. A magnified image is formed at the focal point of eye piece. This is an inverted image. When this image is seen through the eye piece we see a real and highly magnified image.

### **4.5.3 Optical microscopy of membrane sample:**

Optika B-600 optical microscope is used for the analysis of membrane samples.



Figure 18 Optika B-600 optical microscope

The membranes are cut into  $1\text{cm}^2$  pieces and analyzed through the microscope.

#### **4.6 Permeation flux:**

The membrane flux is defined as volume of the fluid flowing through the membrane per unit area per unit time. Its unit is  $\text{m}^3/\text{m}^2.\text{sec}$ . Membrane flux test was performed using the vacuum filtration assembly at constant pressure of 480psi at room temperature. Area of membrane was  $0.025\text{m}^2$ .

Flux = flow rate/area \* time

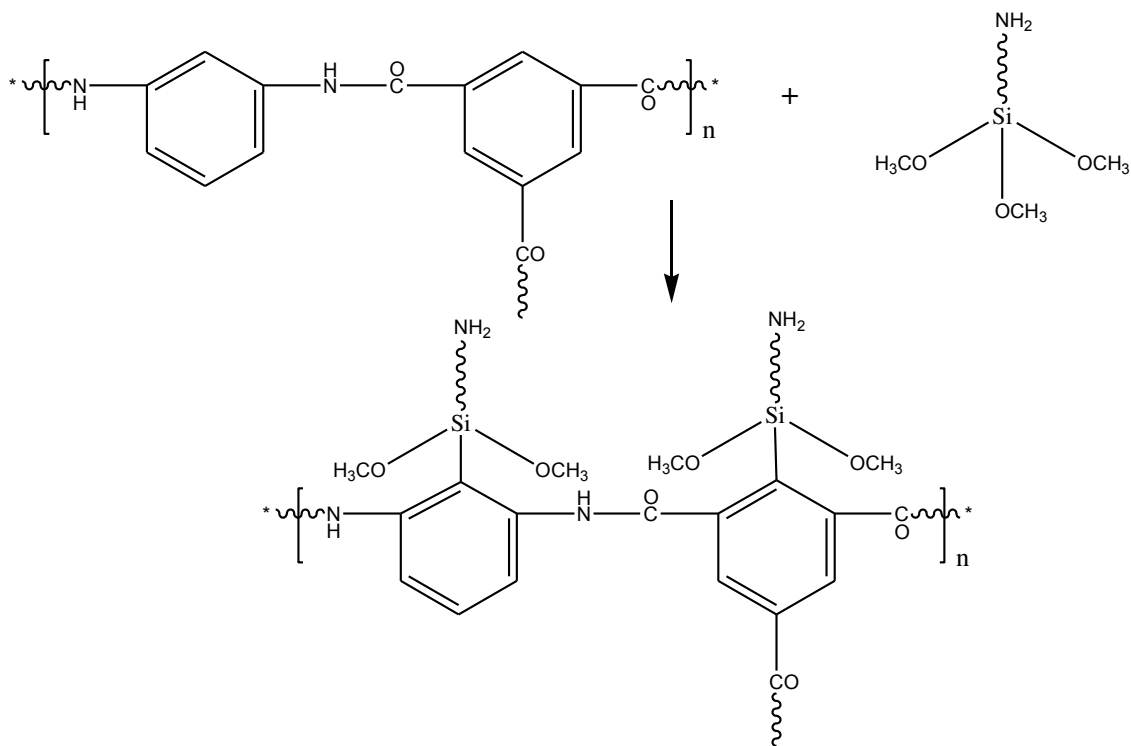
Flow rate= initial volume – final volume.

# CHAPTER 5: Results and discussions

## 5.1: Reaction scheme for the synthesis of polymer brushes:

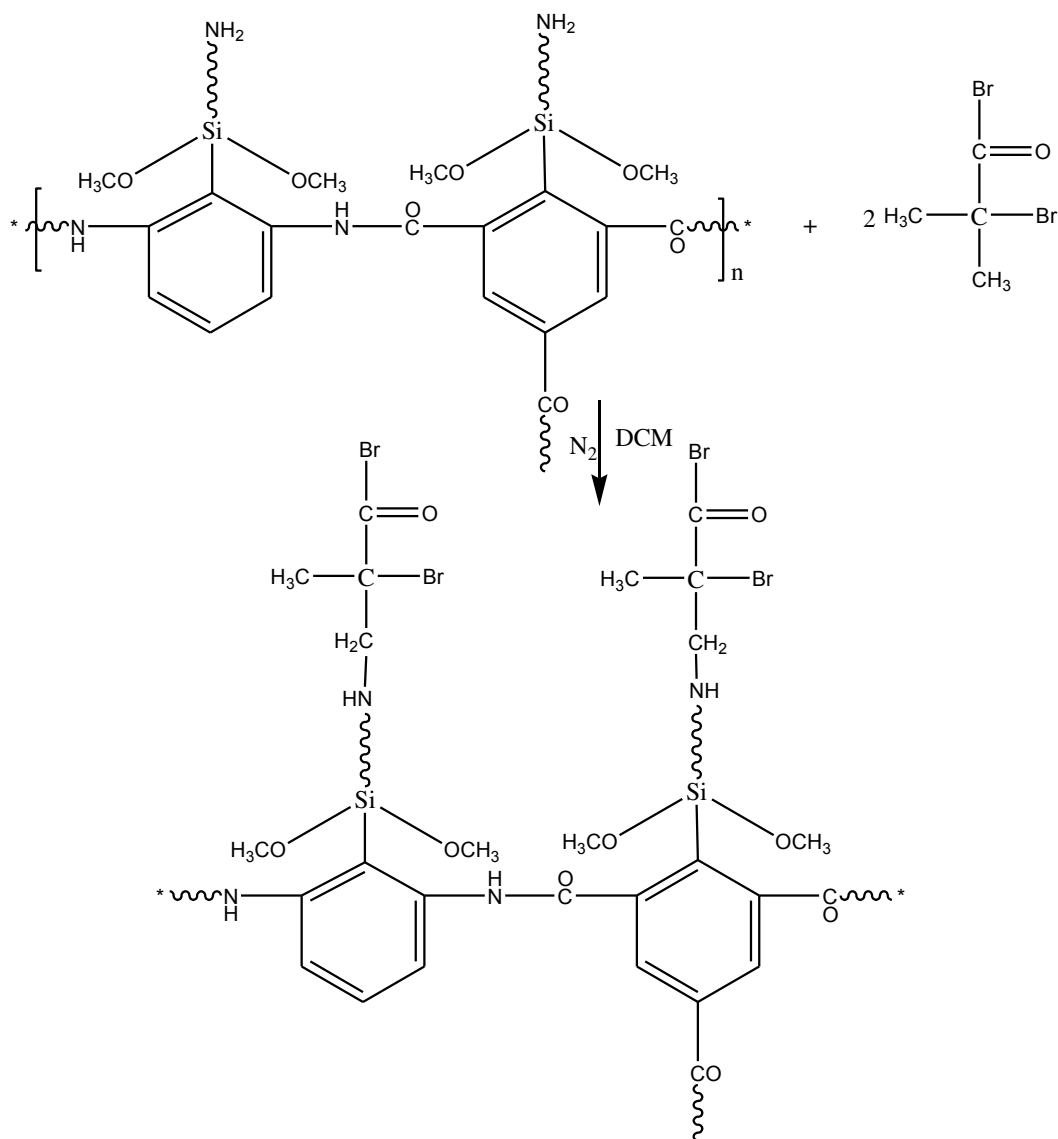
### 5.1.1 Reaction of TFC PA membrane with APTMS:

APTMS reacts with the TFC-PA membrane in which the Si-O-C bond is formed between the silicon atom of APTMS and the carbonyl carbon present in the polyamide chain. Also Si-O-Si bond is formed between the APTMS attached on the polyamide thus forming a coating.



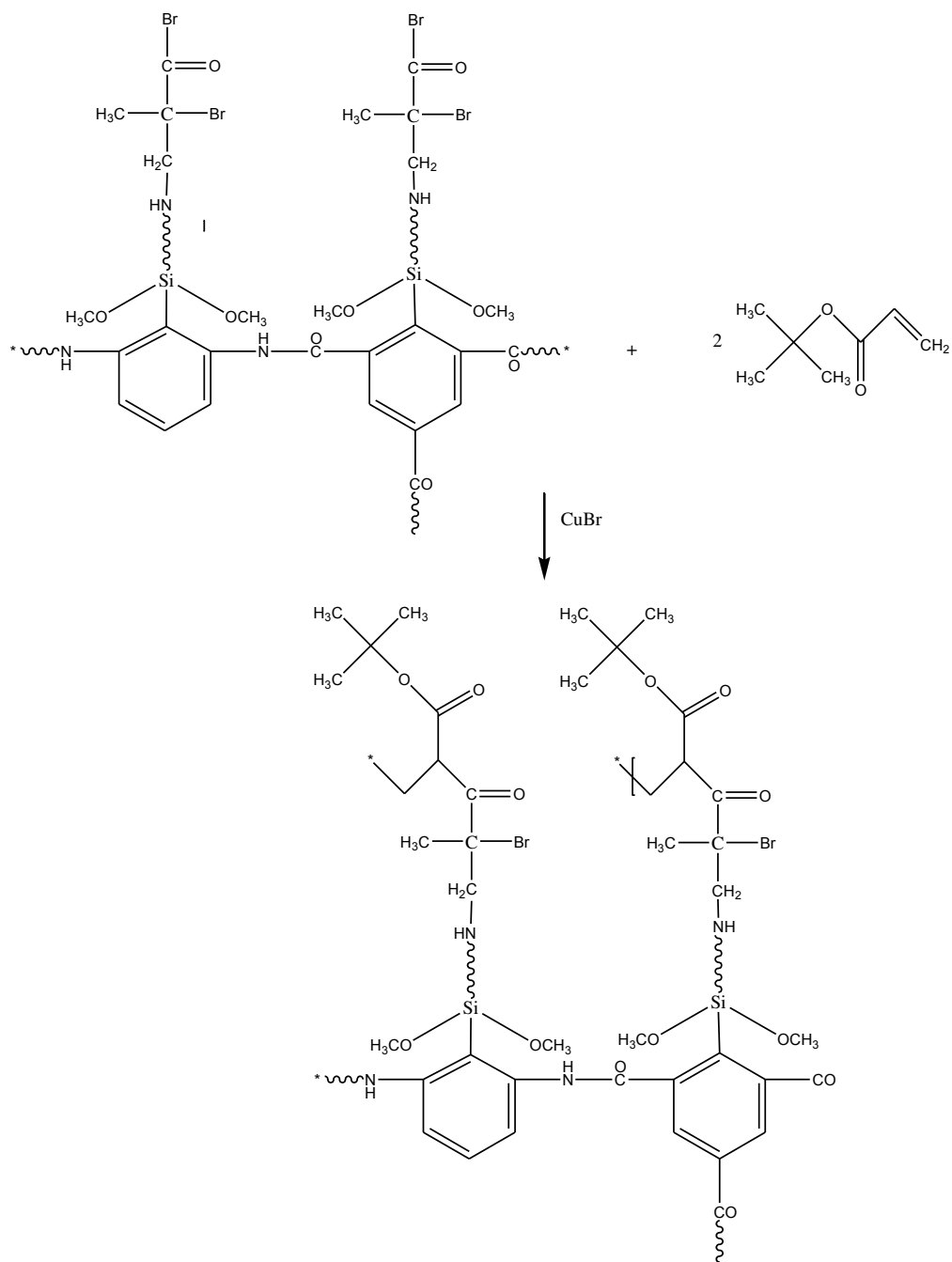
### 5.1.2 Reaction of $\alpha$ -bromo isobutyl with APTMS functionalized TFC PA membrane:

The amine group on the APTMS functionalized PA serve as the reactive center.  $\alpha$ -bromo isobutyl bromide reacts with amine group present on the top of APTMS functionalized polyamide membrane. Thus a bromine atom exposed which serve active specie for ATRP.



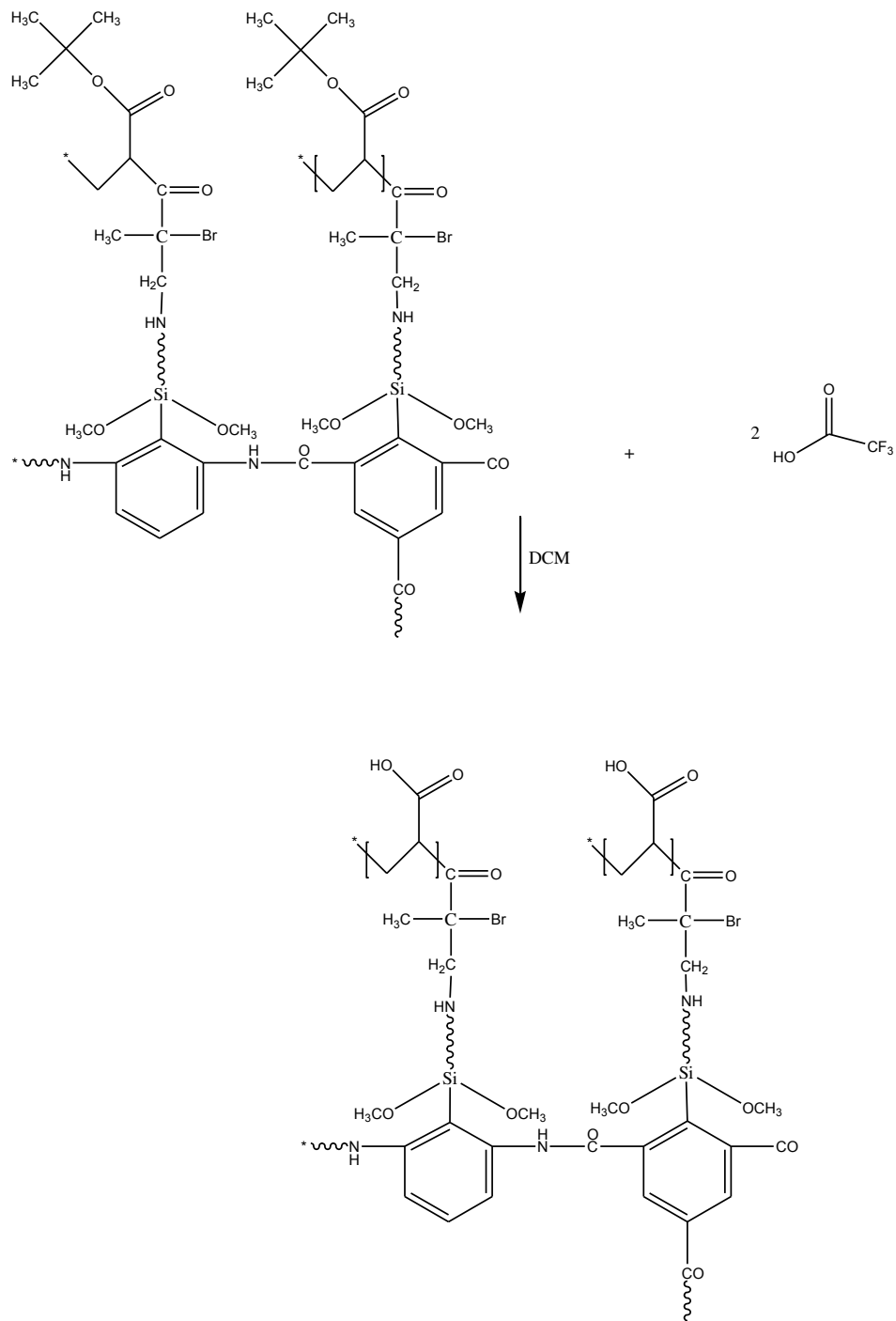
### 5.1.3 PtBA brushes growth on bromide functionalized membrane:

Bromine functionalized polyamide membrane undergoes ATRP in the presence of CuBr(I) and PMDETA and results in the controlled polymerization of t-butyl acrylate onto the polyamide membrane in the form of PtBA brushes.



#### **5.1.4 Hydrolysis of PtBA brushes grown TFC PA membrane:**

As the PtBA is hydrophobic, to make it hydrophilic the PtBA has to be hydrolyzed. Hydrolysis has been achieved by the reaction of trifluoro acetic acid with the PtBA grown membrane. The t-butyl group present the brushes has been hydrolyzed to carboxylic acid group, thus converting PtBA to PAA (polyacrylic acid).



## 5.2 Optical Microscopy analysis:

The optical microscopy has been used to visualize the proceedings of the reaction. First membrane shows the surface morphology of the simple reverse osmosis membrane. Second figure shows the membrane after treatment with APTMS. The third one is



obtained after the initiator attachment over the APTMS functionalized membrane. The fourth one is the polymer brushes grown membrane. It is obvious from the figure that the polymer brushes have been grown over the membrane surface. Thus, it has been concluded that the polymer brushes have been grown successfully on the TFC-PA membrane by ATRP. It has also been concluded that there is the controlled growth of polymer brushes which is the aim of ATRP.

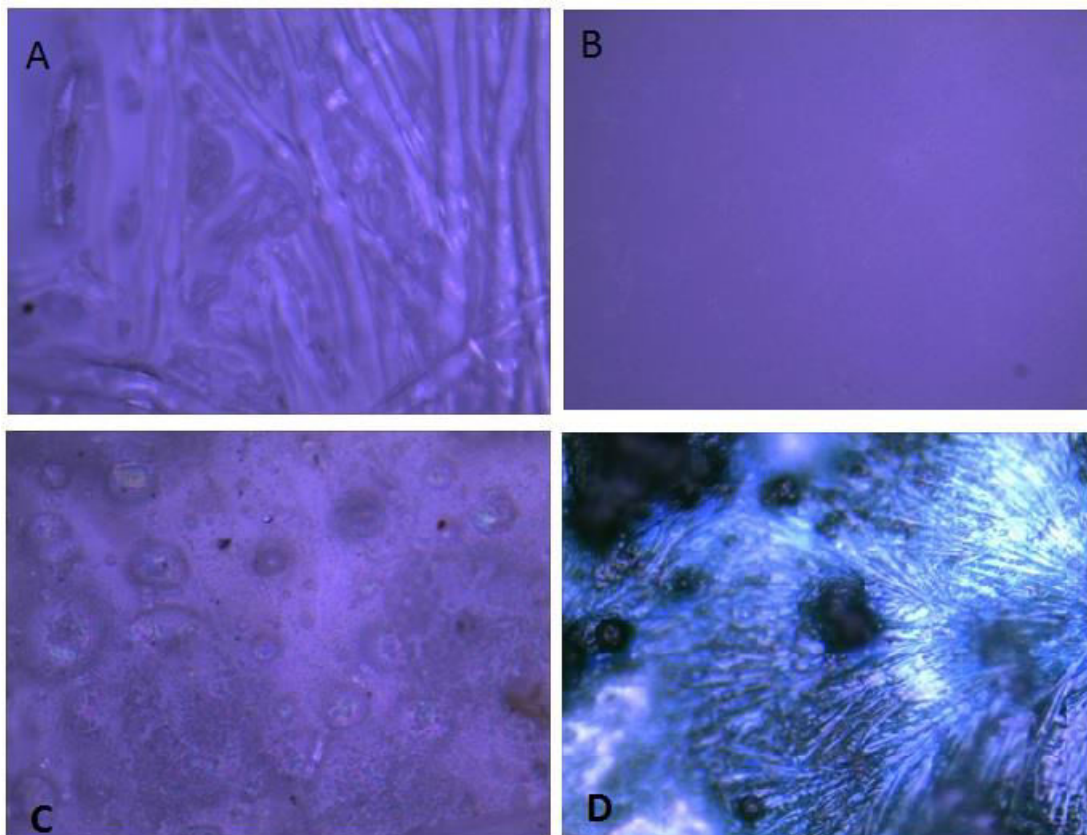
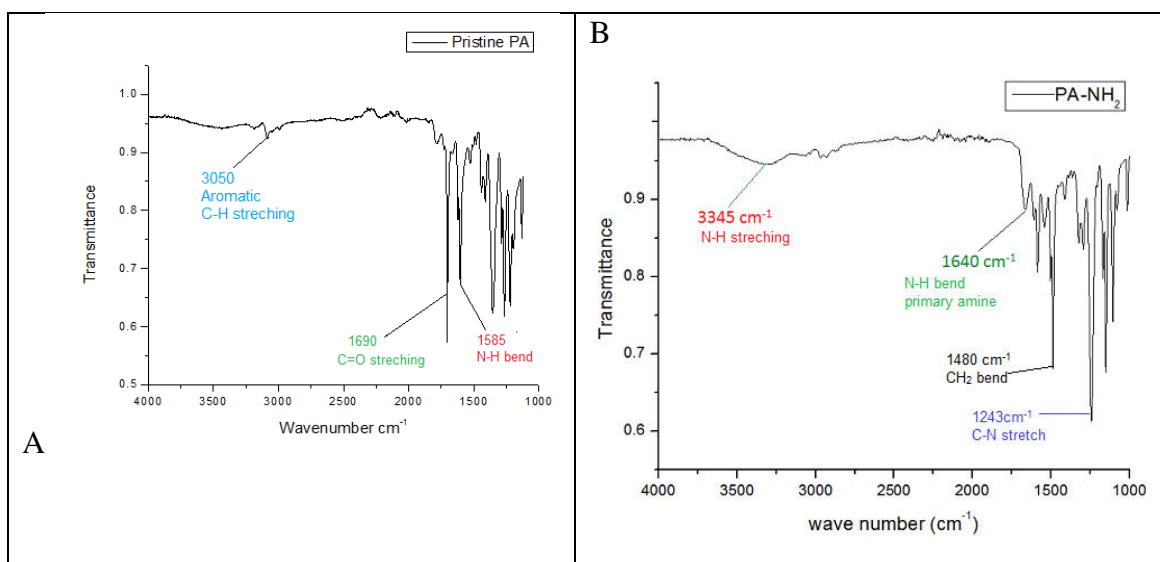


Figure 19 Optical microscopy of a) simple membrane b) TFC PA—NH<sub>2</sub> c) TFC PA---Br d) TFC PA – PtBA brushes.

### 5.3 FTIR-ATR:

Figure 20 shows the FTIR spectra of PA, PA-NH<sub>2</sub>, PA-Br and PA-PtBA membranes. Figure 20(A) shows the FTIR of the pristine PA, the peak at 3050 cm<sup>-1</sup> shows the aromatic stretching which is due to the aromatic group in polyamide, the peak at

1690 $\text{cm}^{-1}$  is designated to C=O and the peak at 1585  $\text{cm}^{-1}$  is that for N-H stretching of the peptide bond present within polyamide structure. Figure 20(B) shows peaks for PA-NH<sub>2</sub>, the peak at 3345  $\text{cm}^{-1}$  is attributed for N-H bond stretching due to presence of amine group, the broad peak results from the weak N-H bond stretching and the peak at 1640 $\text{cm}^{-1}$  is due to the N-H bond bending. It is the sharp peak which means that the extensive bending has occurred in the bond. The peak at 1480 $\text{cm}^{-1}$  shows the CH<sub>2</sub> bend which is due to CH<sub>2</sub> group present in the attached APTMS chain. Figure 20(C) shows The spectra for PA-Br shows that the peak which are formed due to N-H stretching and bending has been disappeared which is due to the conversion of PA-NH<sub>2</sub> to PA-Br, moreover the peak at 1712  $\text{cm}^{-1}$  shows C=O present in the attached  $\alpha$ -bromo isobutyl bromide. For PA-g-PtBA, the peak at 1728  $\text{cm}^{-1}$  is dedicated for C=O group, the peaks from 2977 $\text{cm}^{-1}$  to 2874 $\text{cm}^{-1}$  represent the alkyl C-H stretching which are weak due to presence of t-butyl group. The peaks at 1366  $\text{cm}^{-1}$  corresponds to asymmetric and symmetric C(CH<sub>3</sub>) stretching respectively[99]–[101].The peak at 1728 $\text{cm}^{-1}$  corresponds to C=O present in the t-BA attached.



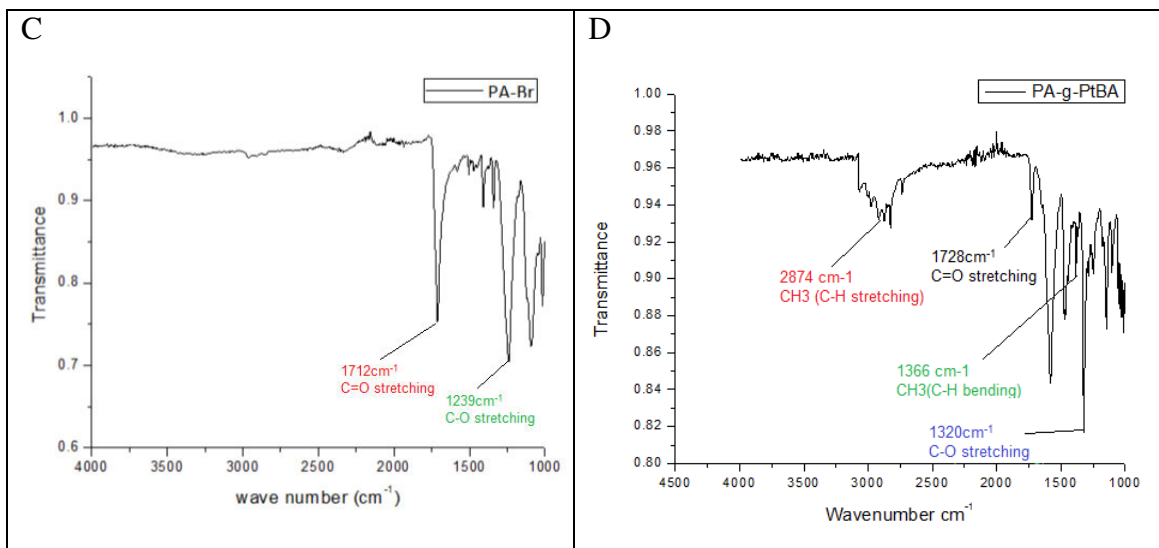


Figure 20 FTIR-ATR analysis of a) PA, b) PA-NH<sub>2</sub>, c) PA-Br, d) PA-g-PtBA

The broad peak at 3185 cm<sup>-1</sup> in figure 21 shows the O-H stretching of the carboxylic group, this broad peak is due to the extensive hydrogen bond in PAA.[102]. The peak at 1780cm-1 is due to C=O present in the carboxylic group.

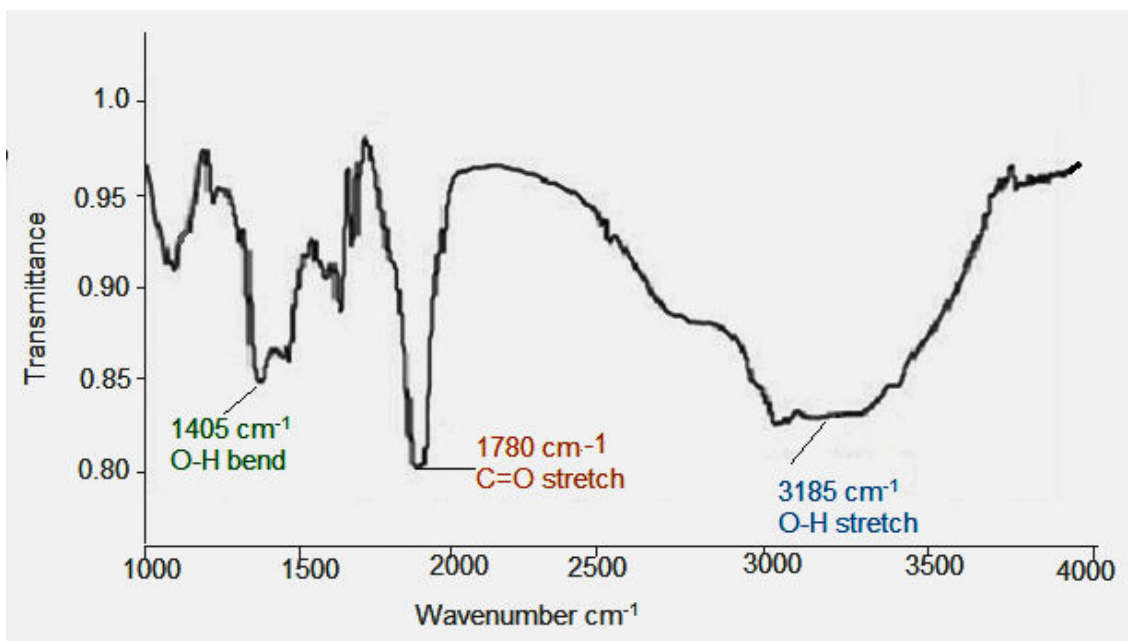


Figure 21 FTIR analysis of TFC PA-PAA

### 5.3 Water contact angle analysis:

Table 2 shows the contact angle of the membranes. This parameter is used for the determination of hydrophilicity/hydrophobicity. the contact angle greater than or equal to  $90^\circ$  is termed as hydrophobic and the material which has contact angle less than  $90^\circ$  is termed as hydrophilic[103]. Figure 22 shows the contact angle of all the membranes. The contact angle TFC-PA, TFC PA-NH<sub>2</sub>, PA-Br, PA-g-PtBA and PA-g-PAA membranes are  $51^\circ$ ,  $57^\circ$ ,  $96^\circ$ ,  $109^\circ$  and  $34^\circ$  respectively. As seen at the contact angles, the minimum contact angle is shown by the PA-g-PAA which is due to the presence of carboxylic acid in PAA which means that it becomes hydrophilic. The maximum contact angle is shown by PA-g-PtBA due to presence of methyl groups. So, we can conclude that the conversion of PA-g-PtBA to PA-g-PAA has greatly reduced the contact angle. The contact angle of PA membrane is  $51^\circ$  and that of PA-PAA membrane is  $34^\circ$  [104]. The contact angle of PAA grafted membrane is less than the commercially available PA membrane, which mean that PA-g- PAA membrane have greater flux commercially existing membrane.

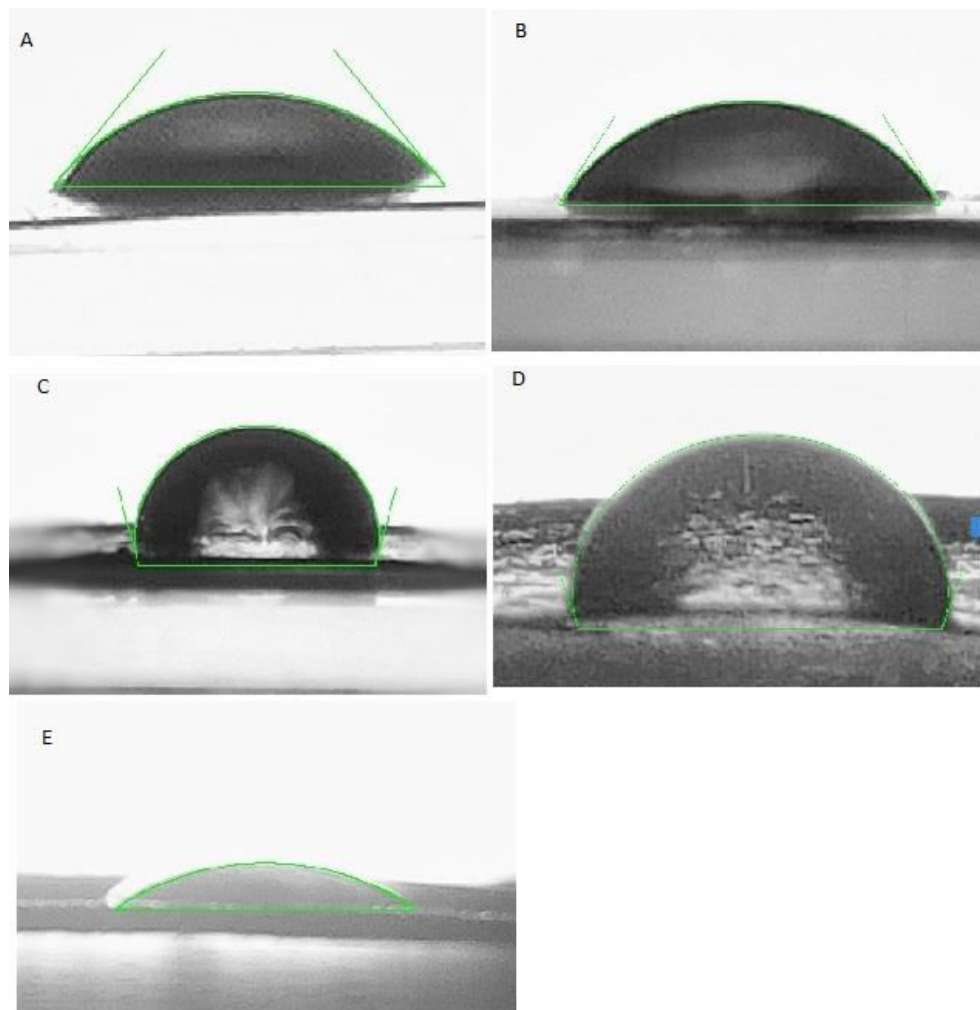


Figure 22 Contact angle images of TFC-PA (A), PA- NH<sub>2</sub> (B), PA-Br(C), PA-g-PtBA (D) and PA-g-PAA (E) membranes.

Sr. No.	Membrane Composition	Average Contact angle
1	TFC-PA	51°
2	PA-NH <sub>2</sub>	57°
3	PA-Br	96°
4	PA-g-PtBA	109°
5	PA-g-PAA	34°

Table 2 Contact angles of the membrane samples

#### **5.4 Scanning electron microscopy SEM:**

Scanning electron microscopy images enables us to determine the morphology, cross-section and average pore size of each membrane. Surface topography and cross-sectional images of the prepared membrane are shown in labeled figures 23 and 24. It is very clear from the SEM images the polymer brushes grown membrane have asymmetric and finger like structure which helps in the better flow properties. The micrographs of the membranes show the remarkable porosity. The pore size ranging from 40 nm to 600nm. So, there is an increase in the pore size of membrane due to the growth of polymer brushes. An important conclusion which can be drawn from the experiment is that the increase in the number of large pores relative to the pure polyamide membrane is due to the growth of polymer brushes onto the membrane. The upright growth of PtBA brushes ease the flow of the water through the membrane. In the previous research, it is clear that by increasing the pore size, porosity and hydrophilicity, wettability and flux is increased.

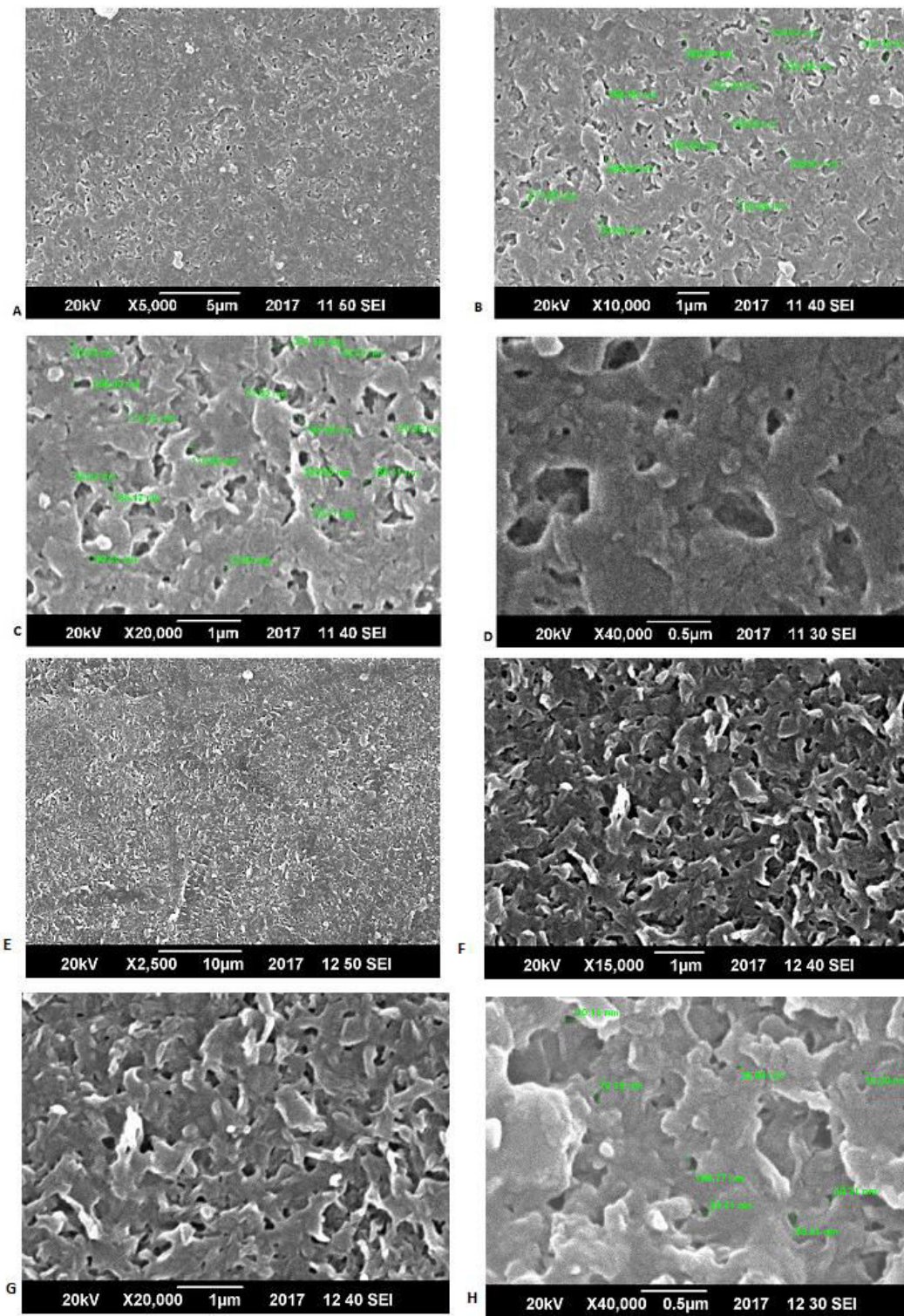


Figure 23 SEM A, B,C and D are surface morphology of PAA-g-PA ,E, F,G and H for simple membrane

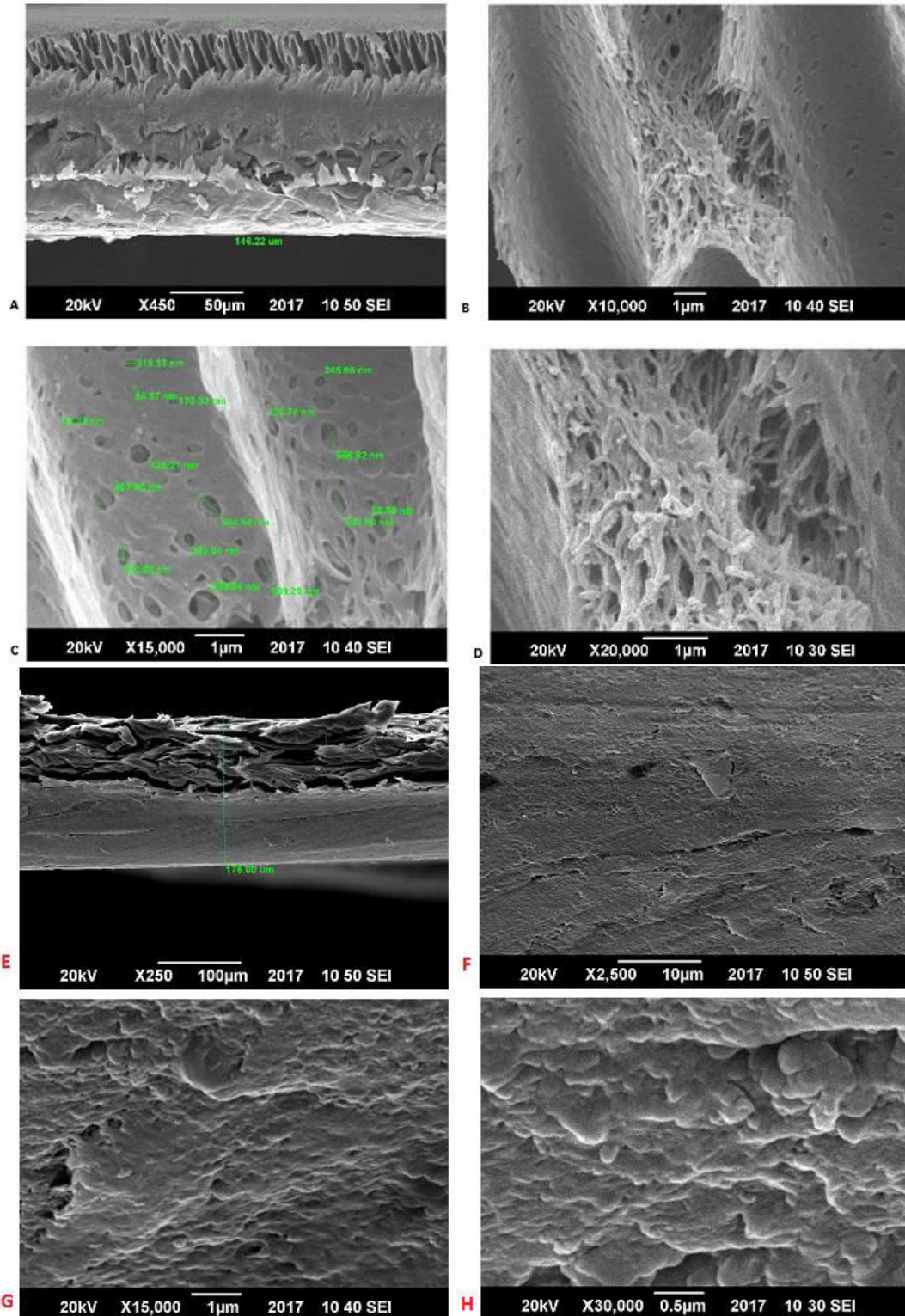


Figure 24 SEM images A, B, C & D cross-section of PAA-g-PA and images E, F, G & H cross-section of simple membrane

### 5.5 Optical profilometry:



Optical profilometry has been used to determine the surface roughness of the PA membrane samples. Roughness is an important parameter for the flux measurements. Hydrophilic surface with degree of roughness will increase the flux through the membrane. From the table 4 it can be seen that the surface roughness has been increased due to the growth of polymer brushes. PA has surface roughness of 40693 nm while PA-g-PtBA membrane has value of 46232 nm which is due to the growth of polymer brushes of PtBA. After the hydrolysis of PA-g-PtBA the PtBA has been converted to PAA, the roughness value has been increased further. This will favor the better flux than the simple PES membrane. So, it can be concluded that due to the growth of PtBA brushes the surface roughness has been increased which increase the flux through the membrane [105].

<b>Sr. No.</b>	<b>Sample Name</b>	<b>Surface Roughness (Ra)</b>
1	TFC-PA	40693nm
2	PA-NH <sub>2</sub>	2284 nm
3	PA-Br	11881 nm
4	PA-g-PtBA	46232 nm
5	PA-g-PAA	47476 nm

Table 3 Surface roughness Ra values of membrane samples.

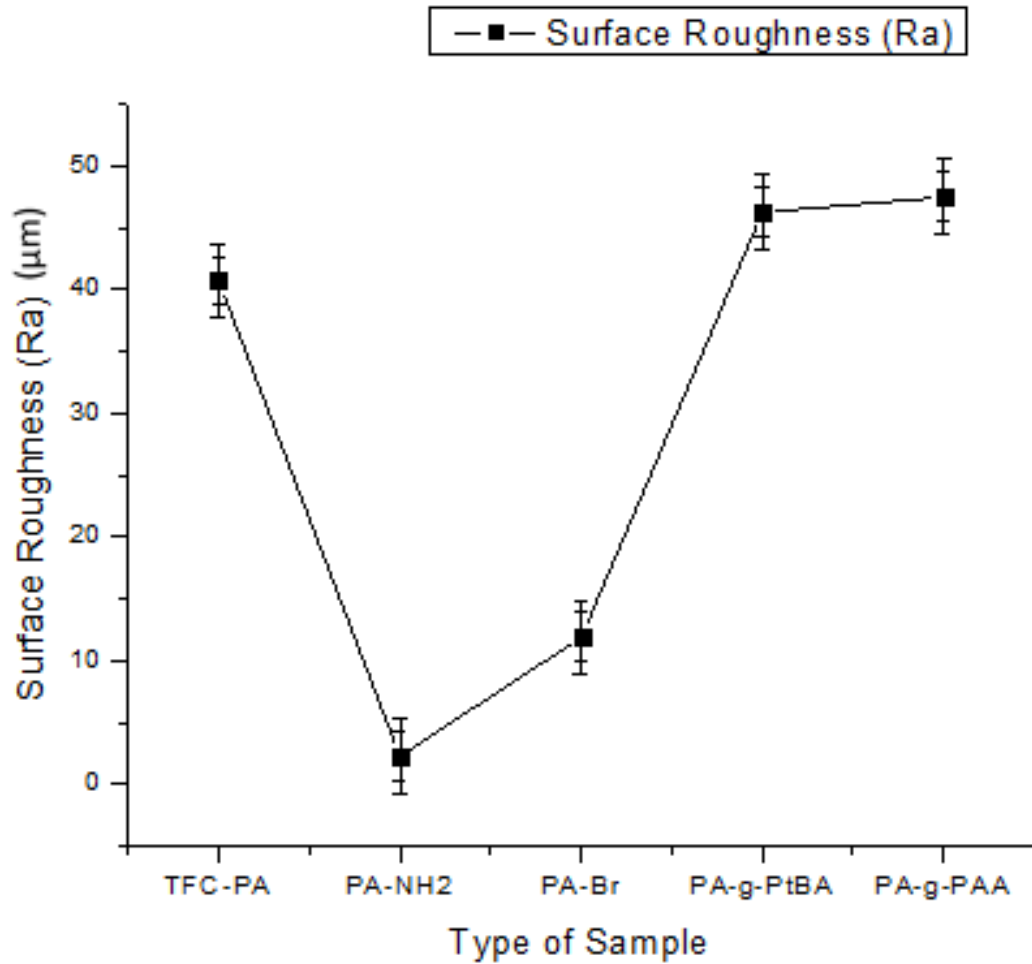


Figure 25 Graph showing the surface roughness values of all samples

### 5.6 Permeation flux:

Water flux through the commercial TFC-PA membrane and PAA grafted TFC-PA membrane was analyzed by using a conventional filtration assembly and results are shown in Figures 26. From the figure it is clear that at lower pH value of 3, membrane shows the maximum flux. The membrane has been subjected to five cycles for flux. And the membrane shows the maximum value for the cycle 5. Permeation flux has been checked at 500 psi. The maximum flux is  $80 \text{ L/m}^2 \cdot \text{hr}$  at the pH value of 3 and the lowest value of flux is  $72 \text{ L/m}^2 \cdot \text{hr}$  at the pH value of 11. Hydrophilicity of the TFC-PA grafted PAA has been considerably increased due to the presence of PAA. The passage of water through the membrane is due to the increase in hydrophilic character. Due to hydrophilic character the water molecules are attracted towards the membrane. Figure

27 show the comparison of flux between modified and neat membrane which shows that the flux of modified membrane was greater than the neat membrane at pH 3 which was due to the increase in hydrophilicity and increase pore size. From the above SEM images, contact angle, pore size and surface roughness, it has already been concluded that due to grafting of PAA on the TFC-PA hydrophilicity of the membrane has improved considerably. Pore size and surface hydrophilicity are the main factors that govern the flux of the membrane.

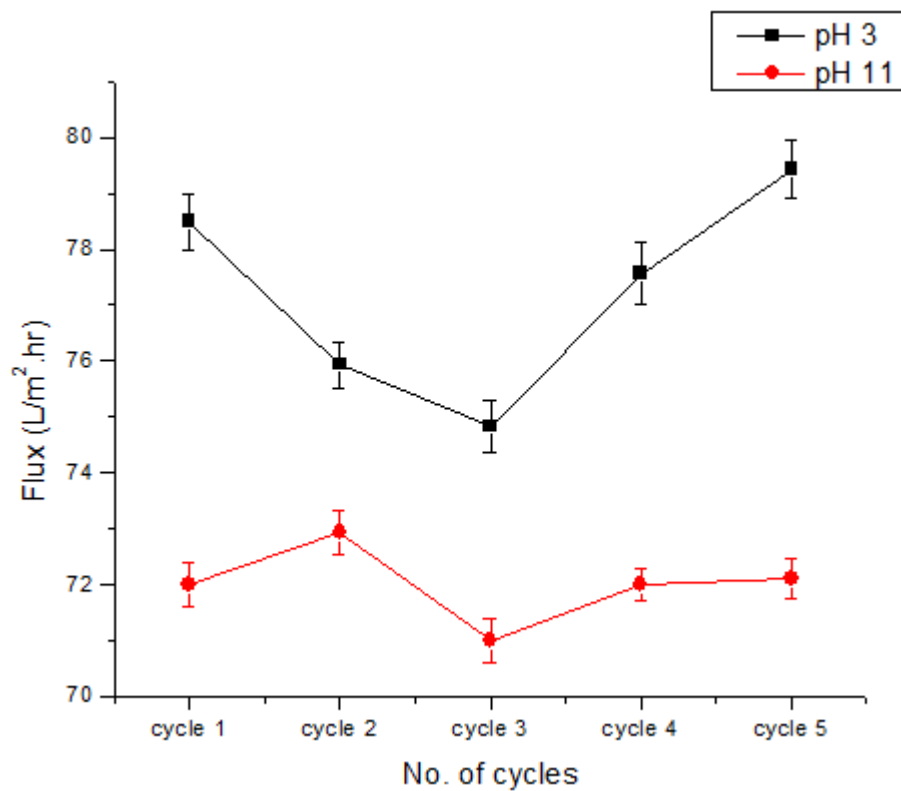


Figure 26 Graph showing the permeation flux for five cycles at pH 3 and 11

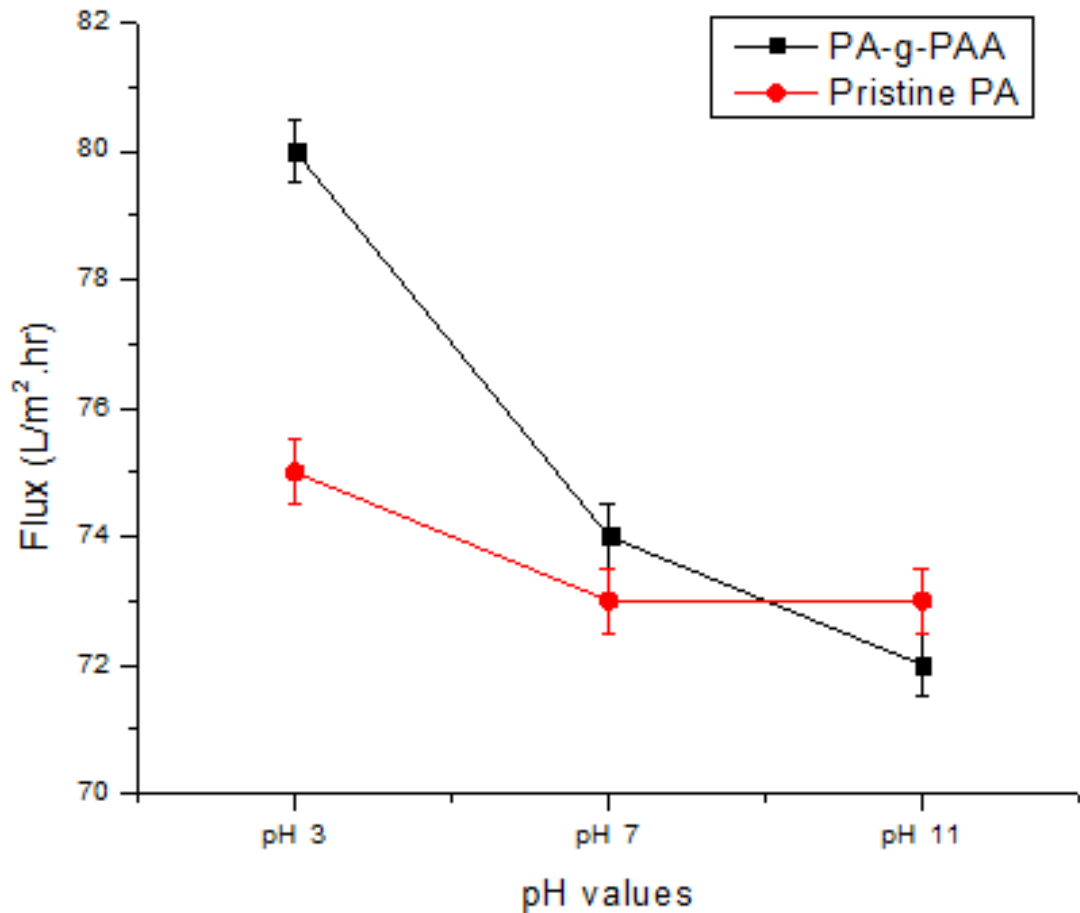


Figure 27 Graph showing the comparison between the fluxes of neat and modified membrane at pH 3 ,7 and 11.

### 5.7 Salt rejection:

Salt rejection is an important feature to analyze the membrane performance as it tells how effectively a membrane can remove contaminants. Range of rejection through RO system is typically 95% to 99%. In the case of desalination, it is referred as salt rejection %.

$$\text{salt rejection \%} = \frac{\text{conductivity of feed water} - \text{conductivity of permeate water}}{\text{conductivity of feed}} * 100$$

The higher the salt rejection, the better the membrane performance. If the membrane has low salt rejection, it means it may require cleaning or replacement. Salt rejection can be calculated from the parameters such as total dissolved solids or conductivity. For the high pressure RO membrane, sodium chloride rejection is often calculated [74].

Salt rejection has been calculated at different pH values. For the experiment 2000ppm solution of NaCl has been used at pH values of 3, 7 and 11. At pH value 3 the membrane shows the maximum value of salt rejection which is 94% [106]. The reason for this value at pH value is due to the presence of an acidic group. This value is somewhat low than the commercial RO membranes which is in the range of 95 to 99.4% but it is in the acceptable range. The slight decrease in the salt rejection is due to the increase in the flux which is 80 L/m<sup>2</sup>.hr for modified membrane but for commercial RO is approx. 50-60 L/m<sup>2</sup>.hr.

<b>Sr. No.</b>	<b>pH value</b>	<b>Permeation flux</b> L/m <sup>2</sup> .hr	<b>% salt rejection</b>
1	3	80	95
2	7	75	92
3	11	72	90

Table 4 Permeation flux and % salt rejection at pH 3 , 7 and 11

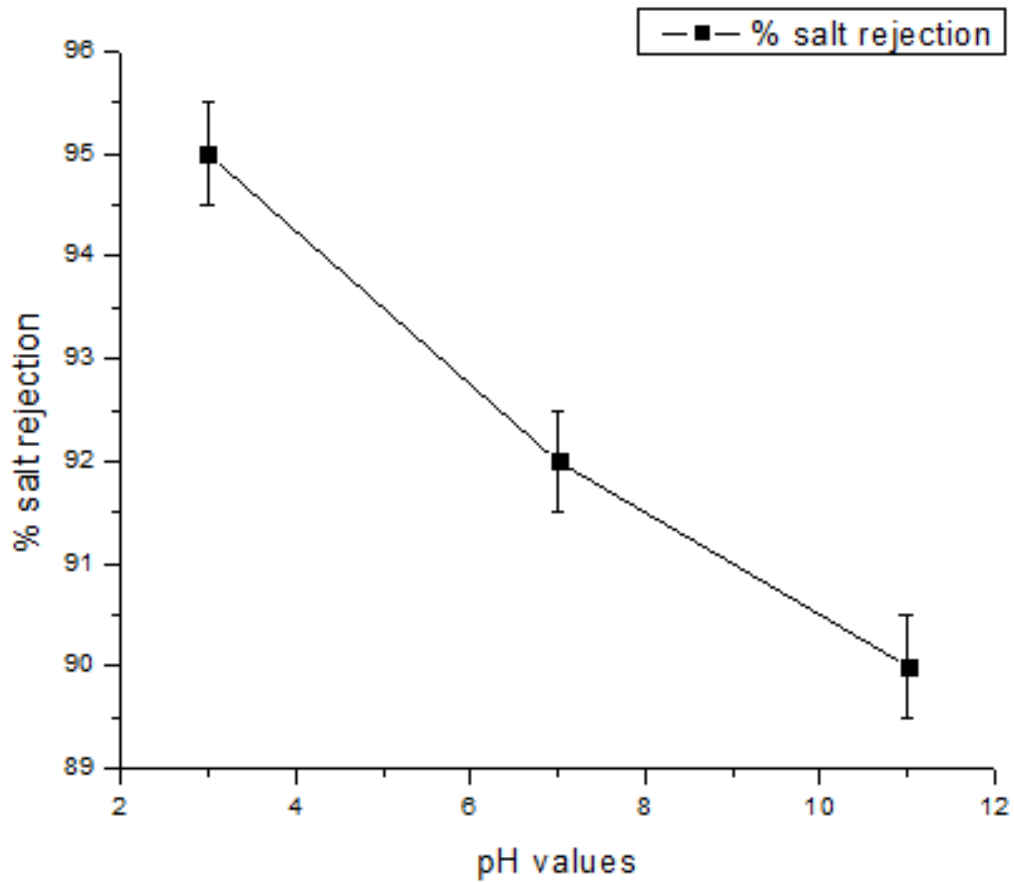


Figure 28 Graph showing the %salt rejection rate

### 5.8 pH responsive behavior of PAA brushes:

The PA-g-PAA membrane shows the reversible and conformational changes to permeability in response to pH changes. These changes help to control the permeability flux at different pH by triggering the pore size[107]–[109]. Protonation and deprotonation of carboxylic group (-COOH) can control the effective pore size of the PA-g- PAA brushes membrane as shown in figure 29. This transformation is sensitive to water pH and results in the swelling and de-swelling of PAA brushes[110].

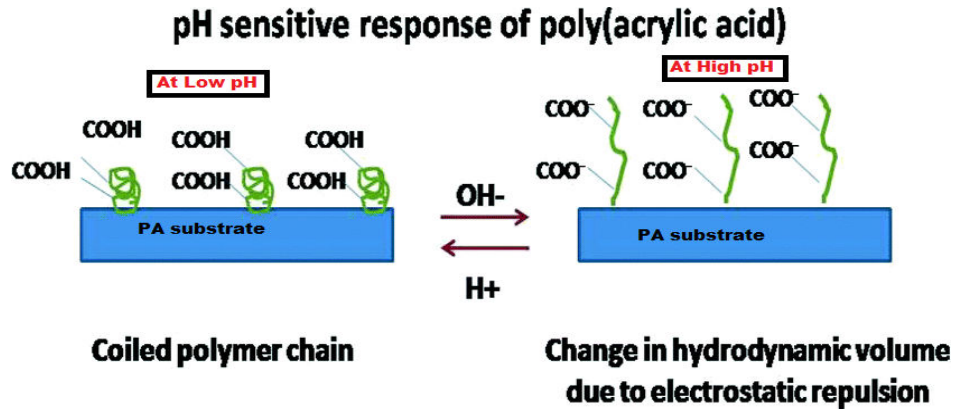


Figure 29 Mechanism of protonation and deprotonation of PAA brushes at low and high pH

At a pH higher than 4 the polyacrylic acid shows the extended conformation, driven from their strong interaction with the aqueous environment and the electrostatic repulsion among the dissociated side chain[111]. The effective pore size is greatly reduced due to these phenomena which in turns declines the permeation flux rate. At low pH the poly acrylic acid chains collapses to form the helical conformation[112]. This effect results in the opening of pores due to which increase in flux is observed as shown in figure 10. The effect of pH on the flux is shown by the model in figure 30.

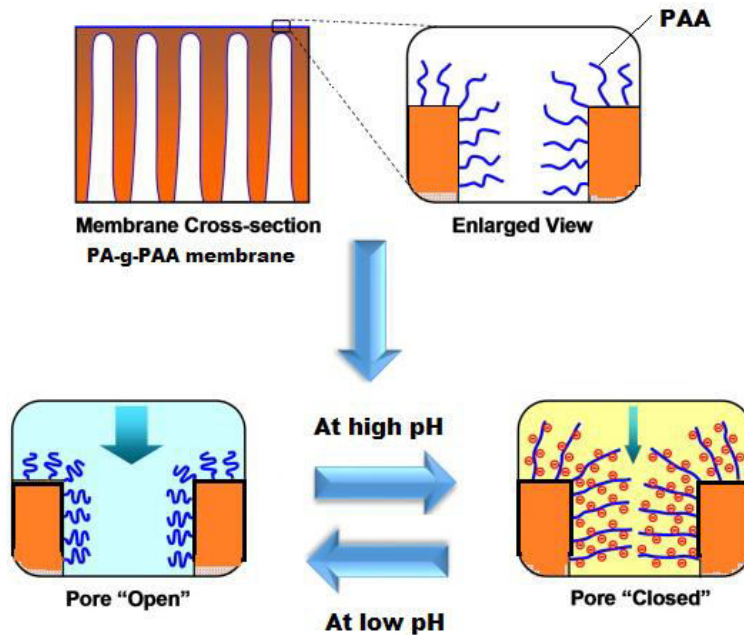


Figure 30 Model showing PAA conformation at low and high pH and its effect on flux

## 5.9 Mechanical Testing

Tensile testing of the membrane has been done with the universal testing machine Shimadzu model AG-X plus. Figure 31 shows the stress-strain curve of both Pristine polyamide and PAA-g-PA membranes. The elastic limit of PAA-g-PA membrane is higher than that of pristine PA which means that is more elastic in nature. The Young's modulus has been calculated by drawing a slope in the elastic region using the formula

$$E = \frac{\sigma e - \sigma o}{\varepsilon e - \varepsilon o}$$

<b>Sample Name</b>	<b>Young's Modulus GPa</b>	<b>UTS MPa</b>	<b>Toughness</b>	<b>%elongation</b>
Pristine PA	5.9±3	64.5±4	976	25
PAA-g-PA	10.6±5	74±5	1069	23

Table 5 : Mechanical properties of pristine PA and PAA-g-PA

The Young's modulus for Pristine PA came out to be  $5.9 \pm 0.4$  GPa and that for PAA-g-PA was  $10.6 \pm 0.35$  GPa which means that due to the grafting of PAA brushes the resistance to deformation of the membrane within the elastic limit has been increased. Also, the value of UTS of PAA grafted membrane is much higher than the pristine PA membrane. Yield point elongation exist in the two curves which is due to the creation of slip band due to stress. The other is due to the presence of impurities.



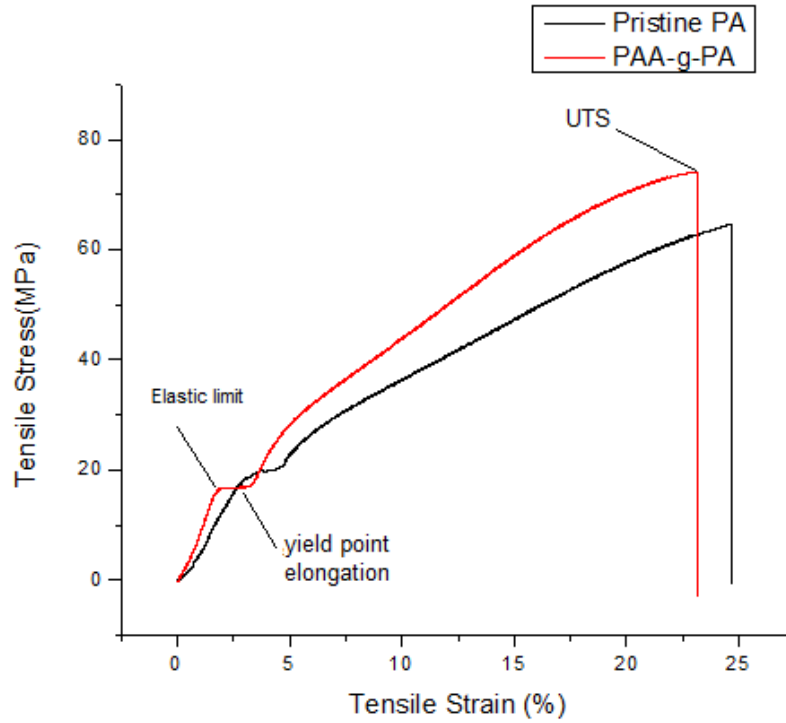


Figure 31 Stress-strain curves of Pristine PA and PAA-g-PA

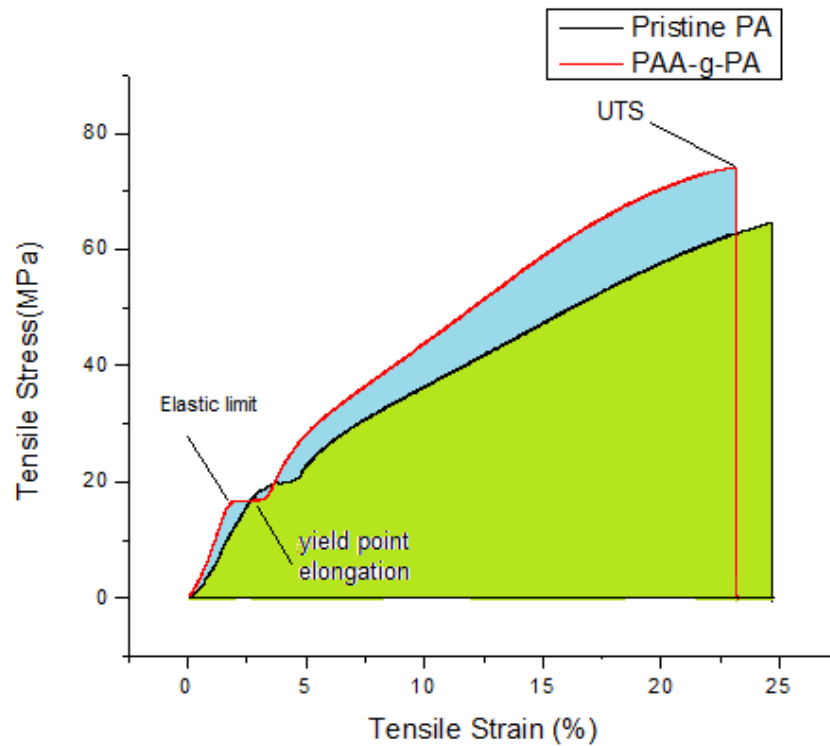


Figure 32 Graph showing the ductility of the Pristine PA and PAA-g-PA

Figure 32 shows the ductility of both membranes. The area under the curve shows the toughness or ductility of the material[113]. From the graph it is clear that due to the grafting of PAA the ductility of the PA membrane has been increased. The growth of polymer brushes form scaffolds due to crosslinking over the surface making it stronger. Moreover the PAA is used as binder and adhesives in many application, so due to this ability of PAA is binds the PA membrane surface strongly therefore the tensile strength distributes more uniformly[110].

# Chapter 6: Conclusions

Polymer brushes of PtBA has been successfully grafted on the commercial TFC-PA through ATRP and the PtBA has been converted to PAA to form the hydrophilic surface. Behavior of the membrane for the flux and salt rejection has been studied. Following conclusions were drawn from this research study.

- 1) Through ATRP method, polymer brushes of PtBA were grown on the membrane surface. Proceeding of the membrane modification was monitored by the contact angle analysis, FTIR, optical microscope and the optical profilometry. The FTIR analysis results confirmed the PtBA and PAA. Salt rejection test was also done to check the performance of membrane.
- 2) Membrane characterization results revealed that grafting of PtBA brushes has remarkable effect on the membrane properties such as porosity, hydrophilicity contact angle and permeation flux was observed. Due to the growth of PtBA brushes the membrane morphology has also been changed.
- 3) Flux of the PAA-g-PA membrane has been considerably increased than the pristine PA membrane
- 4) Hydrophilicity has been increased due to the grafting of PAA
- 5) Switchable performance of PAA-g-PA membrane at different pH's
- 6) Salt rejection testing on the modified membrane was done to investigate the membrane performance. It was done at different pH values. The maximum salt rejection was observed at pH value of 3.

## 6.1 Future recommendation:

- Polymer brushes of different polymer can be grafted on the membrane surface and can be examined.
- By adjusting the flux rate, salt rejection rate can be enhanced.

- This method of polymer brushes growth can be used to graft the membrane surface for antifouling polymer.
- Effect of pH on the surface morphology of the prepared membranes
- Effect of temperature, pressure and mechanical values on the modified membrane
- Study of antifouling properties
- Study for investigating the performance of membrane for seawater and brackish water

# Chapter 7: References

- [1] M. Kummu *et al.*, “The world’s road to water scarcity: Shortage and stress in the 20th century and pathways towards sustainability,” *Sci. Rep.*, vol. 6, no. December, pp. 1–16, 2016.
- [2] CliffNotes.com, “Water Quality Tests,” pp. 13–23, 2011.
- [3] A. Azizullah, M. Nasir, K. Khattak, P. Richter, and D. Häder, “Water pollution in Pakistan and its impact on public health — A review,” *Environ. Int.*, vol. 37, no. 2, pp. 479–497, 2011.
- [4] “7 Water Sustainability in Pakistan – Key Issues and Challenges,” 2015.
- [5] Nestlé, “Nestlé response to Nils Rosemann report ‘Drinking Water Crisis in Pakistan and the Issue of Bottled Water - The Case of Nestlé’s Pure Life,’” no. April, p. 3, 2005.
- [6] F. Nabeela *et al.*, “Microbial contamination of drinking water in Pakistan—a review,” *Environ. Sci. Pollut. Res.*, vol. 21, no. 24, pp. 13929–13942, 2014.
- [7] K. Kowalczyk, T. Spychaj, and G. Krala, “High-build alkyd urethane coating materials with a partially solvolyzed waste polyurethane foam,” *Polym. Eng. Sci.*, vol. 55, no. 9, pp. 2174–2183, 2015.
- [8] R. Field, “Fundamentals of Fouling,” *Membr. Technol.*, vol. 4, pp. 1–23, 2010.
- [9] A. C. M. Franken, “Prevention and control of membrane fouling: practical implications and examining recent innovations,” *Prev. Control Membr. Fouling*, no. June, p. 47, 2009.
- [10] S. Jeon *et al.*, “The effect of membrane material and surface pore size on the fouling properties of submerged membranes,” *Water (Switzerland)*, vol. 8, no. 12, 2016.
- [11] E. M. Vrijenhoek, S. Hong, and M. Elimelech, “Influence of membrane surface properties on initial rate of colloidal fouling of reverse osmosis and nanofiltration

- membranes,” vol. 188, pp. 115–128, 2001.
- [12] D. A. and A. K. Wardani, “Modification and Applications of Hydrophilic Polypropylene Membrane,” *IOP Conf. Ser. Mater. Sci. Eng.*, vol. 214, no. 1, p. 12014, 2017.
- [13] S. Mondal and S. R. Wickramasinghe, “Produced water treatment by nanofiltration and reverse osmosis membranes,” *J. Memb. Sci.*, vol. 322, no. 1, pp. 162–170, 2008.
- [14] A. Drews, “Membrane fouling in membrane bioreactors-Characterisation, contradictions, cause and cures,” *J. Memb. Sci.*, vol. 363, no. 1–2, pp. 1–28, 2010.
- [15] J. M. Arnal, B. García-fayos, and M. Sancho, “Membrane Cleaning,” 2009.
- [16] S. Mondal, “Stimuli Responsive Surfaces for Fouling-resistant Polymeric Membranes,” *J. Membr. Sci. Technol.*, vol. 4, no. 1, pp. 1–2, 2013.
- [17] A. Abdelrasoul, H. Doan, and A. Lohi, “Fouling in Membrane Filtration and Remediation Methods,” *Mass Transf. - Adv. Sustain. Energy Environ. Oriented Numer. Model.*, 2013.
- [18] A. F. Products and P. Information, “Technical Information,” vol. 49, no. 3, pp. 1–2, 2009.
- [19] B. Van Der Bruggen, C. Vandecasteele, T. Van Gestel, W. Doyen, and R. Leysen, “A review of pressure-driven membrane processes in wastewater treatment and drinking water production,” *Environ. Prog.*, vol. 22, no. 1, pp. 46–56, 2003.
- [20] S. P. Beier, *Electrically Driven Membrane Processes*. 2012.
- [21] R. Controlled and S. Processes, “MEMBRANE SEPARATIONS,” 2016.
- [22] M. O. Nigam, B. Bansal, and X. D. Chen, “Fouling and cleaning of whey protein concentrate fouled ultrafiltration membranes,” *Desalination*, vol. 218, no. 1–3, pp. 313–322, 2008.

- [23] Minnesota Rural Water Association, "Chapter19: Membrane Filtration," *Minnesota Water Work. Oper. Man.*, pp. 1–12, 2001.
- [24] W. R. Bowen and H. Mukhtar, "Characterization and prediction of separation performance of nanofiltration membranes.," *J. Memb. Sci.*, vol. 112, no. 2, pp. 263–274, 1996.
- [25] G. Perm, "H. K. Shon et al.: Nanofiltration for water and wastewater treatment," 2013.
- [26] K. P. Lee, T. C. Arnot, and D. Mattia, "A review of reverse osmosis membrane materials for desalination-Development to date and future potential," *J. Memb. Sci.*, vol. 370, no. 1–2, pp. 1–22, 2011.
- [27] J. Cadotte, "Reverse osmosis membrane," *US Pat. 4259183*, 1977.
- [28] J. Cadotte, "United States Patent 4,039,440; Reverse Osmosis Membrane," *US Pat. 4,039,440*, 1977.
- [29] B. M. Ganesh, A. M. Isloor, and M. Padaki, "Preparation and characterization of polysulfone and modified poly isobutylene-alt-maleic anhydride blend NF membrane," *Desalination*, vol. 287, no. February 2016, pp. 103–108, 2012.
- [30] M. KabschKorbutowicz and T. Winnicki, "Application of modified polysulfone membranes to the treatment of water solutions containing humic substances and metal ions," *Desalination*, vol. 105, no. 1–2, pp. 41–49, 1996.
- [31] J. Su, Q. Yang, J. F. Teo, and T. S. Chung, "Cellulose acetate nanofiltration hollow fiber membranes for forward osmosis processes," *J. Memb. Sci.*, vol. 355, no. 1–2, pp. 36–44, 2010.
- [32] J. J. Qin, Y. Li, L. S. Lee, and H. Lee, "Cellulose acetate hollow fiber ultrafiltration membranes made from CA/PVP 360 K/NMP/water," *J. Memb. Sci.*, vol. 218, no. 1–2, pp. 173–183, 2003.
- [33] W.-L. Chou, D.-G. Yu, and M.-C. Yang, "The preparation and characterization of silver-loading cellulose acetate hollow fiber membrane for water treatment,"

*Polym. Adv. Technol.*, vol. 16, no. 8, pp. 600–607, 2005.

- [34] N. Hu, T. Xiao, X. Cai, L. Ding, Y. Fu, and X. Yang, “Preparation and characterization of hydrophilically modified PVDF membranes by a novel nonsolvent thermally induced phase separation method,” *Membranes (Basel)*, vol. 6, no. 4, pp. 1–16, 2016.
- [35] K. Y. Wang, T. S. Chung, and M. Gryta, “Hydrophobic PVDF hollow fiber membranes with narrow pore size distribution and ultra-thin skin for the fresh water production through membrane distillation,” *Chem. Eng. Sci.*, vol. 63, no. 9, pp. 2587–2594, 2008.
- [36] J. R. Du, S. Peldszus, P. M. Huck, and X. Feng, “Modification of poly(vinylidene fluoride) ultrafiltration membranes with poly(vinyl alcohol) for fouling control in drinking water treatment,” *Water Res.*, vol. 43, no. 18, pp. 4559–4568, 2009.
- [37] H. Yanagishita, C. Maejima, D. Kitamoto, and T. Nakane, “Preparation of asymmetric polyimide membrane for water/ethanol separation in pervaporation by the phase inversion process,” *J. Memb. Sci.*, vol. 86, no. 3, pp. 231–240, 1994.
- [38] W. Sun, J. Liu, H. Chu, and B. Dong, “Pretreatment and membrane hydrophilic modification to reduce membrane fouling,” *Membranes (Basel)*, vol. 3, no. 3, pp. 226–241, 2013.
- [39] S. Velu, L. Muruganandam, and G. Arthanareeswaran, “Preparation and performance studies on polyethersulfone ultrafiltration membranes modified with gelatin for treatment of tannery and distillery wastewater,” *Brazilian J. Chem. Eng.*, vol. 32, no. 1, pp. 179–189, 2015.
- [40] E. Celik, H. Park, H. Choi, and H. Choi, “Carbon nanotube blended polyethersulfone membranes for fouling control in water treatment,” *Water Res.*, vol. 45, no. 1, pp. 274–282, 2011.
- [41] A. Ghaee, M. Shariaty-Niassar, J. Barzin, and A. F. Ismail, “Chitosan / Polyethersulfone Composite Nanofiltration Membrane for Industrial Wastewater Treatment,” *Int. J. Nanosci. Nanotechnol.*, vol. 9, no. 4, pp. 213–220, 2013.



- [42] X. Zhang, C. Xiao, and X. Hu, "Preparation and properties of polysulfone/polyacrylonitrile blend membrane and its modification with hydrolysis," *Desalin. Water Treat.*, vol. 51, no. 19–21, pp. 3979–3987, 2013.
- [43] K. Nouzaki *et al.*, "Preparation of polyacrylonitrile ultrafiltration membranes for wastewater treatment," *Desalination*, vol. 144, no. 1–3, pp. 53–59, 2002.
- [44] I. C. Kim, H. G. Yun, and K. H. Lee, "Preparation of asymmetric polyacrylonitrile membrane with small pore size by phase inversion and post-treatment process," *J. Memb. Sci.*, vol. 199, no. 1, pp. 75–84, 2002.
- [45] I. Thus and I. The, "Advanced. materials," *Adv. Mater.*, vol. 148, no. 11, pp. 7–12, 1994.
- [46] D. Rana and T. Matsuura, "Surface modifications for antifouling membranes," *Chem. Rev.*, vol. 110, no. 4, pp. 2448–2471, 2010.
- [47] Y. Mansourpanah, S. S. Madaeni, A. Rahimpour, Z. Kheirollahi, and M. Adeli, "Changing the performance and morphology of polyethersulfone/polyimide blend nanofiltration membranes using trimethylamine," *Desalination*, vol. 256, no. 1–3, pp. 101–107, 2010.
- [48] C. Zhao, J. Xue, F. Ran, and S. Sun, "Modification of polyethersulfone membranes - A review of methods," *Prog. Mater. Sci.*, vol. 58, no. 1, pp. 76–150, 2013.
- [49] B. Fang *et al.*, "Modification of polyethersulfone membrane by grafting bovine serum albumin on the surface of polyethersulfone/poly(acrylonitrile-co-acrylic acid) blended membrane," *J. Memb. Sci.*, vol. 329, no. 1–2, pp. 46–55, 2009.
- [50] A. Hamza, V. A. Pham, T. Matsuura, and J. P. Santerre, "Development of membranes with low surface energy to reduce the fouling in ultrafiltration applications," *J. Memb. Sci.*, vol. 131, no. 1–2, pp. 217–227, 1997.
- [51] Z. Liu *et al.*, "BSA-modified polyethersulfone membrane: preparation, characterization and biocompatibility.," *J. Biomater. Sci. Polym. Ed.*, vol. 20, no. 3, pp. 377–97, 2009.

- [52] C. Zhao, X. Liu, S. Rikimaru, M. Nomizu, and N. Nishi, "Surface characterization of polysulfone membranes modified by DNA immobilization," *J. Memb. Sci.*, vol. 214, no. 2, pp. 179–189, 2003.
- [53] F. Furtado A. A. M. and A. S. Gomes, "Copolymerization of Styrene onto Polyethersulfone Films Induced By Gamma Ray Irradiation.," *Polym. Bull. (Heidelberg, Ger.)*, vol. 57, no. 4, pp. 415–421, 2006.
- [54] A. Schulze, B. Marquardt, M. Went, A. Prager, and M. R. Buchmeiser, "Electron beam-based functionalization of polymer membranes," *Water Sci. Technol.*, vol. 65, no. 3, pp. 574–580, 2012.
- [55] D. S. Wavhal and E. R. Fisher, "Hydrophilic modification of polyethersulfone membranes by low temperature plasma-induced graft polymerization," *J. Memb. Sci.*, vol. 209, no. 1, pp. 255–269, 2002.
- [56] M. L. Steen, A. C. Jordan, and E. R. Fisher, "Hydrophilic modification of polymeric membranes by low temperature H<sub>2</sub>O plasma treatment," *J. Memb. Sci.*, vol. 204, no. 1–2, pp. 341–357, 2002.
- [57] N. Saxena, C. Prabhavathy, S. De, and S. DasGupta, "Flux enhancement by argon-oxygen plasma treatment of polyethersulfone membranes," *Sep. Purif. Technol.*, vol. 70, no. 2, pp. 160–165, 2009.
- [58] L. J. Mu and W. Z. Zhao, "Hydrophilic modification of polyethersulfone porous membranes via a thermal-induced surface crosslinking approach," *Appl. Surf. Sci.*, vol. 255, no. 16, pp. 7273–7278, 2009.
- [59] Y. C. Lin, C. A. Brayfield, J. C. Gerlach, J. Peter Rubin, and K. G. Marra, "Peptide modification of polyethersulfone surfaces to improve adipose-derived stem cell adhesion," *Acta Biomater.*, vol. 5, no. 5, pp. 1416–1424, 2009.
- [60] A. Kulkarni, D. Mukherjee, and W. N. Gill, "Flux enhancement by hydrophilization of thin film composite reverse osmosis membranes," *J. Memb. Sci.*, vol. 114, no. 1, pp. 39–50, 1996.
- [61] M. C. Wilbert, J. Pellegrino, and A. Zydney, "Bench-scale testing of surfactant-

- modified reverse osmosis/nanofiltration membranes,” *Desalination*, vol. 115, no. 1, pp. 15–32, 1998.
- [62] H. Choi, J. Park, T. Tak, and Y. N. Kwon, “Surface modification of seawater reverse osmosis (SWRO) membrane using methyl methacrylate-hydroxy poly(oxyethylene) methacrylate (MMA-HPOEM) comb-polymer and its performance,” *Desalination*, vol. 291, pp. 1–7, 2012.
- [63] P. Taylor, H. Dong, L. Zhang, and H. Chen, “Desalination and Water Treatment Preparation and characterization of surface- modified zeolite-polyamide thin film nanocomposite membranes for desalination Preparation and characterization of surface-modified zeolite-polyamide,” *Desalin. Water Treat.*, no. March 2013, pp. 37–41, 2012.
- [64] T. H. A. Ngo, D. T. Nguyen, K. D. Do, T. T. Minh Nguyen, S. Mori, and D. T. Tran, “Surface modification of polyamide thin film composite membrane by coating of titanium dioxide nanoparticles,” *J. Sci. Adv. Mater. Devices*, vol. 1, no. 4, pp. 468–475, 2016.
- [65] H. J. Kim *et al.*, “High-performance reverse osmosis CNT/polyamide nanocomposite membrane by controlled interfacial interactions,” *ACS Appl. Mater. Interfaces*, vol. 6, no. 4, pp. 2819–2829, 2014.
- [66] P. Wen *et al.*, “Polyamide thin film composite nanofiltration membrane modified with acyl chlorided graphene oxide,” *J. Memb. Sci.*, vol. 535, pp. 208–220, 2017.
- [67] H. Hachisuka, “Composite reverse osmosis membrane having a separation layer with polivinyl alcohol coating and method of reverse osmotic treatment of water.,” *United States Pat.*, vol. 1, no. 19, pp. 1–6, 2001.
- [68] H. Wu *et al.*, “A novel semi-aromatic polyamide TFC reverse osmosis membrane fabricated from a dendritic molecule of trimesoylamidoamine through a two-step amine-immersion mode,” *RSC Adv.*, vol. 7, no. 62, pp. 39127–39137, 2017.
- [69] G. N. B. Baroña, J. Lim, M. Choi, and B. Jung, “Interfacial polymerization of polyamide-aluminosilicate SWNT nanocomposite membranes for reverse

- osmosis,” *Desalination*, vol. 325, pp. 138–147, 2013.
- [70] T. Hong Anh Ngo, S. Mori, and D. Thi Tran, “Photo-induced grafting of poly(ethylene glycol) onto polyamide thin film composite membranes,” *J. Appl. Polym. Sci.*, vol. 134, no. 43, pp. 1–9, 2017.
- [71] R. Reis *et al.*, “Charge tunable thin-film composite membranes by gamma-ray triggered surface polymerization,” *Sci. Rep.*, vol. 7, no. 1, p. 4426, 2017.
- [72] E. F. Castro Vidaurre, C. A. Achete, R. A. Simão, and A. C. Habert, “Surface modification of porous polymeric membranes by RF-plasma treatment,” *Nucl. Instruments Methods Phys. Res. Sect. B Beam Interact. with Mater. Atoms*, vol. 175–177, pp. 732–736, 2001.
- [73] R. Reis *et al.*, “Amine Enrichment of Thin-Film Composite Membranes via Low Pressure Plasma Polymerization for Antimicrobial Adhesion,” *ACS Appl. Mater. Interfaces*, vol. 7, no. 27, pp. 14644–14653, 2015.
- [74] I. Vidalis, “Surface hydrophilic modification of RO membranes by plasma polymerization for low organic fouling,” *Charact.*, vol. 1, 2010.
- [75] E. J. Bodner *et al.*, “Attachment of antimicrobial peptides to reverse osmosis membranes by Cu(I)-catalyzed 1,3-dipolar alkyne-azide cycloaddition,” *RSC Adv.*, vol. 6, no. 94, pp. 91815–91823, 2016.
- [76] Q. Shi, Y. Su, X. Ning, W. Chen, J. Peng, and Z. Jiang, “Trypsin-enabled construction of anti-fouling and self-cleaning polyethersulfone membrane,” *Bioresour. Technol.*, vol. 102, no. 2, pp. 647–651, 2011.
- [77] G. Kang and Y. Cao, “Development of antifouling reverse osmosis membranes for water treatment: A review,” *Water Res.*, vol. 46, no. 3, pp. 584–600, 2012.
- [78] L. Li, G. Yan, J. Wu, X. Yu, and Q. Guo, “Functionalization of Poly(ether imide) Membranes via Surface-Initiated Atom-Transfer Radical Polymerization and their Use in Antifouling,” *High Perform. Polym.*, vol. 21, no. 4, pp. 455–467, 2009.

- [79] Y. Zhang, Z. Wang, W. Lin, H. Sun, L. Wu, and S. Chen, "A facile method for polyamide membrane modification by poly(sulfobetaine methacrylate) to improve fouling resistance," *J. Memb. Sci.*, vol. 446, pp. 164–170, 2013.
- [80] K. Matyjaszewski, "Atom Transfer Radical Polymerization and the Synthesis of Polymeric Materials," *Adv. Mater.*, vol. 10, no. 12, pp. 901–915, 1998.
- [81] K. Matyjaszewski and J. Xia, "Atom transfer radical polymerization.," *Chem. Rev.*, vol. 101, no. 9, pp. 2921–2990, 2001.
- [82] V. Coessens, T. Pintauer, and K. Matyjaszewski, "Functional polymers by atom transfer radical polymerization," *Prog. Polym. Sci.*, vol. 26, no. 3, pp. 337–377, 2001.
- [83] K. Matyjaszewski and N. V. Tsarevsky, "Nanostructured functional materials prepared by atom transfer radical polymerization," *Nat. Chem.*, vol. 1, no. 4, pp. 276–288, 2009.
- [84] N. V. Tsarevsky, P. McCarthy, W. Jakubowski, J. Spanswick, and K. Matyjaszewski, "Atom transfer radical polymerization (ATRP) as a tool for the synthesis of well-defined functional polymeric materials," *Tech. Proc. 2008 NSTI Nanotechnol. Conf. Trade Show, NSTI-Nanotech, Nanotechnol. 2008*, vol. 2, pp. 665–668, 2008.
- [85] T. Pintauer and K. Matyjaszewski, "Atom transfer radical addition and polymerization reactions catalyzed by ppm amounts of copper complexes," *Chem. Soc. Rev.*, vol. 37, no. 6, p. 1087, 2008.
- [86] M. Horn and K. Matyjaszewski, "Solvent Effects on the Activation Rate Constant in Atom Transfer Radical Polymerization," *Macromol. (Washington, DC, U. S.)*, vol. 46, no. 9, pp. 3350–3357, 2013.
- [87] S. T. Milner, "Polymer Brushes," *Science (New York, N.Y.)*, vol. 251, no. 4996, pp. 905–914, 1991.
- [88] B. Zhao and W. J. Brittain, "Polymer brushes: Surface-immobilized macromolecules," *Prog. Polym. Sci.*, vol. 25, no. 5, pp. 677–710, 2000.

- [89] R. Barbey *et al.*, “Polymer brushes via surface-initiated controlled radical polymerization: synthesis, characterization, properties, and applications,” *Chem. Rev.*, vol. 109, no. Copyright (C) 2012 American Chemical Society (ACS). All Rights Reserved., pp. 5437–5527, 2009.
- [90] S. Yamamoto, M. Ejaz, Y. Tsujii, M. Matsumoto, and T. Fukuda, “Controlled Graft Polymerisation of Methyl Methacrylate on Silicon Substrate by the combined use of the Langmuir-Blodgett and Atom Transfer Radical Polymerisation Techniques,” *Macromolecules*, vol. 31, no. 17, pp. 5934–5936, 1998.
- [91] S. Edmondson, V. L. Osborne, and W. T. S. Huck, “Polymer brushes via surface-initiated polymerizations,” *Chem. Soc. Rev.*, vol. 33, no. 1, p. 14, 2004.
- [92] F. Seeliger and K. Matyjaszewski, “Temperature effect on activation rate constants in ATRP: New mechanistic insights into the activation process,” *Macromolecules*, vol. 42, no. 16, pp. 6050–6055, 2009.
- [93] A. T. Nguyen, J. Baggerman, J. M. J. Paulusse, C. J. M. Van Rijn, and H. Zuilhof, “- Stable Protein-Repellent Zwitterionic Polymer Brushes Grafted from Silicon Nitride,” - *Langmuir*, no. 6, p. 2587, 2011.
- [94] S. H. Lee *et al.*, “Polymer brushes via controlled, surface-initiated atom transfer radical polymerization (ATRP) from graphene oxide,” *Macromol. Rapid Commun.*, vol. 31, no. 3, pp. 281–288, 2010.
- [95] C. Liu, J. Lee, J. Ma, and M. Elimelech, “Antifouling Thin-Film Composite Membranes by Controlled Architecture of Zwitterionic Polymer Brush Layer,” *Environ. Sci. Technol.*, vol. 51, no. 4, pp. 2161–2169, 2017.
- [96] L. Sun, G. L. Baker, and M. L. Bruening, “Polymer brush membranes for pervaporation of organic solvents from water,” *Macromolecules*, vol. 38, no. 6, pp. 2307–2314, 2005.
- [97] M. L. Bruening, D. M. Dotzauer, P. Jain, L. Ouyang, and G. L. Baker, “Creation of functional membranes using polyelectrolyte multilayers and polymer brushes,”

- Langmuir*, vol. 24, no. 15, pp. 7663–7673, 2008.
- [98] N. Ayres, S. G. Boyes, and W. J. Brittain, “Stimuli-responsive polyelectrolyte polymer brushes prepared via atom-transfer radical polymerization,” *Langmuir*, vol. 23, no. 1, pp. 182–189, 2007.
- [99] S. Matsumura *et al.*, “Ionomers for proton exchange membrane fuel cells with sulfonic acid groups on the end-groups: Novel branched poly(ether-ketone)s,” *Am. Chem. Soc. Polym. Prepr. Div. Polym. Chem.*, vol. 49, no. 1, pp. 511–512, 2008.
- [100] B. Li, Y. Shi, W. Zhu, Z. Fu, and W. Yang, “Synthesis of Amphiphilic Polystyrene-*b*-Poly(acrylic acid) Diblock Copolymers by Iodide-Mediated Radical Polymerization,” *Polym. J.*, vol. 38, no. 4, pp. 387–394, 2006.
- [101] T. Wu, J. Genzer, P. Gong, I. Szleifer, P. Vlcek, and V, “Behavior of surface-anchored poly (acrylic acid) brushes with grafting density gradients on,” *brushes Synth. Character. Appl.*, pp. 8756–8764, 2004.
- [102] X. Pang, L. Zhao, M. Akinc, J. K. Kim, and Z. Lin, “Novel amphiphilic multi-arm, star-like block copolymers as unimolecular micelles,” *Macromolecules*, vol. 44, no. 10, pp. 3746–3752, 2011.
- [103] K.-Y. Law, “Definitions for Hydrophilicity, Hydrophobicity, and Superhydrophobicity: Getting the Basics Right,” *J. Phys. Chem. Lett.*, vol. 5, no. 4, pp. 686–688, 2014.
- [104] A. Mourran, W. Tillmann, H. Keul, and M. Chemistry, “Protective Layer for Hydrophilic Self Cleaning Glass,” pp. 3369–3384, 2010.
- [105] S. H. Woo, J. Park, and B. R. Min, “Relationship between permeate flux and surface roughness of membranes with similar water contact angle values,” *Sep. Purif. Technol.*, vol. 146, pp. 187–191, 2015.
- [106] B. Khorshidi, T. Thundat, B. A. Fleck, and M. Sadrzadeh, “A novel approach toward fabrication of high performance thin film composite polyamide membranes,” *Sci. Rep.*, vol. 6, no. February, pp. 1–10, 2016.

- [107] M. K. Sinha and M. K. Purkait, "Preparation and characterization of novel pegylated hydrophilic pH responsive polysulfone ultrafiltration membrane," *J. Memb. Sci.*, vol. 464, pp. 20–32, 2014.
- [108] Z. Han *et al.*, "Toward robust pH-responsive and anti-fouling composite membranes via one-pot in-situ cross-linked copolymerization," *Desalination*, vol. 349, pp. 80–93, 2014.
- [109] T. Luo *et al.*, "PH-responsive poly(ether sulfone) composite membranes blended with amphiphilic polystyrene-block-poly(acrylic acid) copolymers," *J. Memb. Sci.*, vol. 450, pp. 162–173, 2014.
- [110] D. M. Davenport, M. Gui, L. R. Ormsbee, and D. Bhattacharyya, "Development of PVDF membrane nanocomposites via various functionalization approaches for environmental applications," *Polymers (Basel)*, vol. 8, no. 2, 2016.
- [111] L. Ferro, O. Scialdone, and A. Galia, "Preparation of pH sensitive poly(vinylidene fluoride) porous membranes by grafting of acrylic acid assisted by supercritical carbon dioxide," *J. Supercrit. Fluids*, vol. 66, pp. 241–250, 2012.
- [112] S. R. Tonge and B. J. Tighe, "Responsive hydrophobically associating polymers: A review of structure and properties," *Adv. Drug Deliv. Rev.*, vol. 53, no. 1, pp. 109–122, 2001.
- [113] K. Wang *et al.*, "Dynamic behavior and flame retardancy of HDPE/hemp short fiber composites: Effect of coupling agent and fiber loading," *Compos. Struct.*, vol. 113, no. 1, pp. 74–82, 2014.